

EAI4CC: Deciphering Lung and Colon Cancer Categorization  
within a Federated Learning Framework Harnessing the  
Power of Explainable Artificial Intelligence

by

Ankhi Akter Mim  
20101365

Kazi Habibul Ashakin  
20101376

Sadat Hossain  
20101367

Nabiha Tasnim Orchi  
20301148

Al Shahriar Him  
20301131

A thesis submitted to the Department of Computer Science and Engineering  
in partial fulfillment of the requirements for the degree of  
B.Sc. in Computer Science

Department of Computer Science and Engineering  
Brac University  
January 2024

© 2024. Brac University  
All rights reserved.

# Declaration

It is hereby declared that

1. The thesis submitted is my/our own original work while completing degree at Brac University.
2. The thesis does not contain material previously published or written by a third party, except where this is appropriately cited through full and accurate referencing.
3. The thesis does not contain material which has been accepted, or submitted, for any other degree or diploma at a university or other institution.
4. We have acknowledged all main sources of help.

## Student's Full Name & Signature:

---

Ankhi Akter Mim  
20101365

---

Kazi Habibul Ashakin  
20101376

---

Sadat Hossain  
20101367

---

Nabiha Tasnim Orchi  
20301148

---

Al Shahriar Him  
20301131

# Approval

The thesis/project titled “EAI4CC: Deciphering Lung and Colon Cancer Categorization within a Federated Learning Framework Harnessing the Power of Explainable Artificial Intelligence” submitted by

1. Ankhi Akter Mim (20101365)
2. Kazi Habibul Ashakin (20101376)
3. Sadat Hossain (20101367)
4. Nabiha Tasnim Orchi (20301148)
5. Al Shahriar Him (20301131)

Of Fall, 2023 has been accepted as satisfactory in partial fulfillment of the requirement for the degree of B.Sc. in Computer Science on January 18, 2024.

## Examining Committee:

Supervisor:  
(Member)

---

Md. Ashraful Alam, PhD  
Associate Professor  
Department of Computer Science and Engineering  
Brac University

Co-Supervisor:  
(Member)

---

Rafeed Rahman  
Lecturer  
Department of Computer Science and Engineering  
Brac University

Program Coordinator:  
(Member)

---

Md. Golam Rabiul Alam, PhD  
Professor  
Department of Computer Science and Engineering  
Brac University

Head of Department:  
(Chair)

---

Sadia Hamid Kazi, PhD  
Chairperson and Associate Professor  
Department of Computer Science and Engineering  
Brac University

# Abstract

Advances between medical imaging and artificial intelligence (AI) have led to improvements in cancer diagnosis and classification. This paper provides a new framework called Explainable AI for cancer categorization (EAI4CC), which has been developed to define lung and colorectal cancer classification in an integrated manner, addressing privacy concerns by enabling collaborative model training using Federated Learning. In this study, EAI4CC used convolutional neural networks (CNNs) such as VGG 16, VGG19, ResNet50, DenseNet121 and Vision Transformer to analyze histopathological images from lung and colon tissue. In Federated Learning architecture it ensures data privacy while enabling model training on dispersed dataset. Furthermore, state-of-the-art artificial intelligence (XAI) presentation techniques are used. In particular gradient-weighted class activation mapping (GradCAM) combined with EAI4CC to elucidate the decision-making process of the model. The evaluation system shows good performance in important evaluation measures such as accuracy, precision, specificity, sensitivity, and F1 score. More importantly, it enhances model interpretation capabilities, explaining each prediction. This gives doctors clarity and confidence in AI-assisted diagnosis. Interpretable and reliable methods allow AI technologies to be responsibly integrated into the critical cancer research workflow to demonstrate the performance of model measures. In summary, this breakthrough sets a standard to establish a framework for AI to achieve more accurate, transparent, and equitable clinical decision-making.

**Keywords:** AI, EAI4CC, Federated Learning, histopathological image, CNNs, VGG 16, VGG19, ResNet50, DenseNet121, Vision Transformer, GradCAM, XAI

## **Acknowledgement**

First of all, we express our gratitude to the Great Almighty for helping us to complete our thesis without any serious setback.

Then, we heartily thank our supervisor, Md. Ashraful Alam, PhD for providing us with his tremendous assistance and guidance. We'd also like to appreciate our co-supervisor, Rafeed Rahman for being there for us wherever we needed.

Finally, without our parent's constant support, it may not be possible. With their awe-inspiring help and prayers, we are currently on the brink of graduating.

# Table of Contents

<b>Declaration</b>	<b>i</b>
<b>Approval</b>	<b>ii</b>
<b>Abstract</b>	<b>iv</b>
<b>Acknowledgment</b>	<b>v</b>
<b>Table of Contents</b>	<b>vi</b>
<b>1 Introduction</b>	<b>2</b>
1.1 Background of Colon Cancer . . . . .	3
1.2 Background of lung cancer . . . . .	4
1.3 Problem statement . . . . .	5
1.4 Research Objective . . . . .	6
1.5 Research Orientation . . . . .	7
1.6 Contribution: . . . . .	8
<b>2 Literature Review</b>	<b>9</b>
<b>3 Methodology</b>	<b>14</b>
3.1 Dataset Description . . . . .	16
3.1.1 Classes of Dataset . . . . .	17
3.2 Data Pre-Processing . . . . .	19
3.2.1 Resizing . . . . .	19
3.2.2 Scaling & Normalization . . . . .	19
3.3 Splitting of the Dataset . . . . .	20
3.3.1 Distribution of the Dataset for CNN models . . . . .	20
3.3.2 Distribution of dataset for FL implementation . . . . .	21
3.4 Used Architectures in Our Research . . . . .	22
3.4.1 VGG16 . . . . .	22
3.4.2 VGG19 . . . . .	23
3.4.3 ResNet50 . . . . .	24
3.4.4 DenseNet121 . . . . .	26
3.4.5 Vision Transformer . . . . .	28
3.4.6 GradCAM . . . . .	29
3.4.7 Federated Learning . . . . .	30
3.5 Experimental Setup . . . . .	31

<b>4</b>	<b>Result Analysis</b>	<b>32</b>
4.1	Performance Measure . . . . .	32
4.2	Performance Analysis of Individual Model . . . . .	33
4.2.1	Learning Curves . . . . .	33
4.2.2	Classification Report . . . . .	36
4.2.3	Confusion Matrix . . . . .	39
4.2.4	Result Analysis & Comparison: . . . . .	42
4.2.5	GradCAM Visualization of Individual Model . . . . .	43
4.3	Performance Evaluation of Federated Learning . . . . .	45
4.3.1	Result Analysis of Global Model . . . . .	45
4.3.2	Learning Curves for Global Model . . . . .	45
4.3.3	Classification Report for Global Model . . . . .	45
4.3.4	Confusion Matrix for Global Model . . . . .	46
4.3.5	ROC Curve for Global Model . . . . .	46
4.3.6	GradCAM Visualization of FL Model . . . . .	47
4.4	The Web Application “EAI4CC” . . . . .	49
<b>5</b>	<b>Conclusion and Future Work</b>	<b>51</b>
	<b>Bibliography</b>	<b>56</b>
	<b>Appendix</b>	<b>57</b>



# Chapter 1

## Introduction

Over the last decade, The death rate from cancer as a whole has dropped. The understanding of how challenging it is to prevent, diagnose, treat, and live with cancer has advanced significantly thanks to research conducted both domestically and internationally. 18.1 million additional instances of cancer are expected to be detected globally by 2020. The following is a breakdown of the numbers: There are 8.8 million women and 9.3 million men. With an additional 1.9 million cases in 2020, breast and lung cancer will rank as the most frequent cancers globally by 2020, accounting for 12.5% and 12.2% of all new cases, respectively. With 10.7% of new cases, colorectal cancer is the third most frequent type of cancer. symbolizes the part[21]. Cancer is still an aggressive and dangerous disease despite advancements in the immune system, the rise of precision medicine, which can improve cancer outcomes to lessen health inequities, research on lymph node dissection, and machine learning approaches to understand flawless data. The use of tissue samples from histopathologic images is crucial for the diagnosis, planning, and assessment of cancer. However, the manual interpretation of these images is influenced by topic content and significance knowledge, which can lead to changes in research. Additionally, the amount of data and the requirement for precise specimen identification may strain human resources, which could have an impact on accuracy. Ensuring the security of picture data in healthcare facilities is crucial for upholding patient confidentiality laws. Through preprocessing, feature extraction, training samples, and cooperation with medical professionals, applied machine learning facilitates the identification of cancer from histopathology images. Furthermore, acknowledging government education as a vital alternative is becoming more and more important. We developed a method to run collaborative machine learning models on decentralized machines without disclosing confidential information. Our approach simulates the training of sensitive partitioned data to simulate a unified model while maintaining strict privacy protection.

The main goal is to develop a system that combines collaborative learning principles, semantics in AI framework, and modern machine learning algorithms. Our intention is to accurately classify and register tissues in histopathology scans of colorectal growth. This strategy also emphasizes the creation of strong and ethical governance for data and AI practices. Using publicly available medical research, the system promotes a more sustainable data privacy policy, as well as helping clinicians better diagnose cancer tissue. We believe this drives the development of AI with conscience

and performance of development in health care is established . The major innovation lies in enabling improvements in the decentralized model and in adhering to privacy principles that are often sacrificed to research advances. We want to make such a commitment to be an integral part of AI development, increasing fairness and accessibility.

## 1.1 Background of Colon Cancer

According to the American Cancer Society (ACS), a reliable source[34], colorectal cancer is the third most frequent form of cancer in the country. When cells in the colon or rectum develops uncontrollably, this condition is known as colorectal cancer. “Colon cancer” is a common abbreviation for this disease. We refer to the final portion of the digestive tract as the colon. The rectum is the tube that links your colon to your urethra. Several things, like genes, diet, toxins in the environment, and bowel diseases that cause inflammation, have been linked to its development. Men and women are equally vulnerable to colon cancer. Colon Cancer is more common in older people, but anyone can get it. The overwhelming majority (over 75%) of cases of colon and rectal cancer occur in people with no identifiable cancer agents, highlighting the significance of routine screening. Colon cancer risk is increased by a personal or family history of the disease and by polyps in the colon. Typically, polyps, or small clumps of cells, form on the lining of the colon first and are completely benign. There is a risk that some polyps will progress to cancer of the colon in the future.

Colon cancer typically begins with DNA changes in otherwise healthy colon cells. A cell’s DNA stores instructions that it uses to carry out its functions. To keep the body running smoothly, healthy cells replicate and proliferate in a controlled manner. On the other hand, when a cell’s DNA is damaged and it develops into cancer, the cells continue to divide even though more cells aren’t required. Tumors develop when abnormal cell growth becomes excessive. Invasion and destruction of healthy tissue by cancer cells is a slow process that takes time. Furthermore, malignant cells can metastasize to other organs and establish deposits there (metastasis). There are a lot of causes for colon cancer. Colon cancer can be diagnosed at any age, however, the majority of individuals are over 50 years old[35]. Colon cancer has been on the rise among adults under the age of 50, but doctors are uncertain as to why. Additionally, African-Americans have a higher colon cancer risk than people of other races. If you’ve previously experienced colorectal cancer or polyps, you’re more likely to develop colon cancer. Inflammatory bowel diseases (IBDs) of the colon, such as ulcerative colitis and Crohn’s disease, have been linked to an increased risk of developing colon cancer. Colon cancer risk can be greatly increased by inherited gene alterations that have been passed down through the generations. Only a fraction of colon cancers are thought to have a genetic component. Lynch syndrome, also known as hereditary nonpolyposis colorectal cancer, and familial adenomatous polyposis (FAP) are the two most frequent genetic syndromes that increase the risk of colon cancer. In addition to a genetic predisposition, a low-fiber, high-fat diet, inactivity, obesity, diabetes, tobacco use, cancer radiation therapy, and other factors can all increase one’s risk of developing colon cancer. Healthcare providers utilize numerous tests to diagnose colon cancer. Examples of such exami-

nations are: Blood cell count and count of all cells in the blood (CBC), Metabolic profile that covers all the bases (CMP), X-rays for the measurement of carcinoembryonic antigen (CEA), CT scan, or computed tomography, MRI scan, or magnetic resonance imaging, PET scan, or positron emission tomography, Ultrasound, Biopsy.

The majority of patients with colon cancer are treated with surgery. Several operations and treatments exist to cure this dangerous colon cancer.

- A polypectomy is a kind of surgery which takes out polyps that could turn into cancer.
- When only a portion of the colon needs to be removed, the procedure is called a resection or partial colectomy.
- When cancer is found in the colon, surgeons remove it along with some good tissue around it. Using a technique termed anastomosis, they will join together functional pieces of the colon.
- Surgery including removal of the affected portion of the colon and subsequent reconnection of the intestines is called a resection with colostomy. The procedure of choice is the colostomy.
- Using radio waves and heat, cancer cells are eliminated during radiofrequency ablation.
- Adjuvant therapy may be used in conjunction with surgery. Pre or post-operative chemotherapy is a cancer treatment option. They may also be useful for treating metastatic or recurrent forms of colon cancer.

## 1.2 Background of lung cancer

In the United States, the second most common cancer is Lung cancer, with approximately 236,740 cases per year after skin cancer[24]. This condition is caused by irregular proliferation of lung cells, and has the potential to spread throughout the body through allergic rhinitis. Most cases, about 85%, are caused by lung cancer not in small cells, leaving the rest with small cell carcinoma[36]. Although it primarily affects individuals 65 years of age and older, lung cancer can present at any age and is a leading cause of cancer-related death, associated with approximately 1 in 4 cases. 5 years of overall survival is about 21%, but early detection significantly improves prognosis, up to 60% [27]

The leading cause of lung cancer death is smoking, which is responsible for 80-90% of deaths related to this particular cancer. Other contributing factors include secondhand smoke, exposure to radiation and asbestos, and a family or personal history of illness that increases the risk of multiple sclerosis. It includes the use of various imaging modalities, including CT, PET, and MRI imaging, as well as microscopic analysis of lung fluid and tissue samples. This comprehensive approach helps identify the type, size, and location of cancer, which is important to guide appropriate treatment. Treatment modalities include surgery (wedge resection, lobe resection,

pneumonectomy), chemotherapy, radiation, and immunotherapy, used individually or in combination, depending on the cancer stage Palliative care is the mainstay their focus for details whose prognosis is poor, aiming to increase comfort and improve quality of life.

New treatments that emphasize the importance of early detection offer hope for better outcomes in the management of lung cancer.

Key aspects of lung cancer treatment:

- Wedge resection removes small abscessed lung segments to preserve healthy tissue
- Lobectomy removes the tumor-containing lobe
- For metastatic cancer, the lung tissue removed the entire lung
- Radiofrequency ablation uses electrical heat to destroy small tumors
- Stereotactic body irradiation precisely targets tumor cells, sparing healthy cells
- Chemotherapy for cancer requires the use of anticancer agents before/after surgery or in combination with radiation
- The immune system stimulates biological mechanisms to fight cancer in the older population
- Targeted therapies inhibit specific lung cancer cell growth pathways
- Palliative care increases comfort when treatment is not possible

### 1.3 Problem statement

Accurate diagnosis of colorectal cancer is a formidable challenge in medical research. Research to address this has focused on two key areas: mitigating privacy concerns through integrated learning, ensuring effective use of sensitive medical information, while encouraging diagnostic confidence based on AI is strengthened by the addition of interpretable AI. Not only does this ensure honest identification, it also provides clear identification, increasing confidence in the potential of AI in the medical community.

Patient delays, especially when it comes to spinal health, compound the issue, leading to delays in diagnosis and aggressive treatment. Overcoming unwanted health problems is crucial for early detection and intervention. While machine learning and deep learning show promise in early cancer detection, ongoing challenges such as labeling healthy cells as cancerous and other misclassifications remain an obstacle.

To overcome these challenges, this research takes a hidden and unknown approach, integrating the development of state-of-the-art products such as Vision Transformer,

DenseNet121, ResNet50, VGG16, VGG19. GradCAM enhances the interpretability of these models. Addressing privacy concerns, integrated learning is being introduced to ensure joint model training without compromising individual dataset privacy, aiming to de-obscure artificial intelligence and create medicalization protection of sensitive information.

In conclusion, accurate diagnosis of colorectal cancer and lung cancer is an important goal. This study not only highlights the importance of early diagnosis and treatment but actively addresses important challenges by applying government education to address privacy concerns. Furthermore, Explainable AI is used from the beginning to increase credibility, providing not only insights but also explanations of insights. This approach not only increases confidence in doctors' abilities, but also helps incorporate AI into medical research in a more transparent and reliable way.

## 1.4 Research Objective

Our aim is to build a privacy protected federated learning framework, named Explainable Cancer AI (EAI4CC), for interpreting lung and colon cancer classifications using deep neural networks from histopathological images. Such as:

- Inspecting the individual performances of the sophisticated models such as VGG16, VGG19, ResNet50, DenseNet121 and Vision transformer.
- Evaluate the performance of the covert approach across crucial metrics, including accuracy, precision, recall, and F1 score, to showcase the model's commendable capabilities in cancer diagnosis.
- Implement cutting-edge Explainable Artificial Intelligence (XAI) methods, specifically Gradient-weighted Class Activation Mapping (GradCAM), to visualize the decision-making process of EAI4CC in analyzing histopathological images.
- Address privacy concerns by integrating a decentralized training prototype, federated learning, to cooperatively train the EAI4CC model across multiple medical facilities without compromising raw data privacy

### **Comprehensive Model Understanding:**

Delve into a thorough understanding of the employed models to discern how they differentiate between histopathological images.

### **Model Evaluation and Selection:**

- Conduct training, validation, and testing phases to comprehensively assess model performance.
- Identify and select the best-performing model based on achieved accuracy.
- Visualization by GradCAM

### **Federated Learning Implementation:**

- Implement federated learning discreetly on the identified best model.
- Ensure that the application of federated learning remains undetected for the preservation of privacy and security.

### **Interpretation of Results:**

- Recognize the critical importance of interpreting results, particularly in life-threatening situations.
- Prioritize gaining insights into how the models interpret and classify the histopathological images accurately.

## **1.5 Research Orientation**

In the next chapters of our paper, we will thoroughly discuss about some specific topics that are given below:

**Literature review:** A literature review establishes the state of knowledge on a subject, identifies areas that need more research, and directs the formulation of research inquiries or hypotheses, laying the groundwork for a research effort. In order to provide the backdrop and conceptual structure for our research, we reviewed more than fifteen related research publications. These reviews helped us show that the researcher is knowledgeable about the field and various theoretical viewpoints.

**Methodology:** The methodology section explains the research process in great depth and enables readers to assess the validity and trustworthiness of the study's conclusions. The following are the subsections of this chapter:

- Dataset description
- Data pre processing
- Splitting of the dataset
- Used architecture in our research
- Experimental setup

**Result analysis:** The summary and interpretation of our data, along with an analysis of the results in light of the research questions and hypotheses we posed in our study, constitute result analysis. Here, the subsections are:

- Performance measure
- Learning curves
- Confusion matrix
- Classification report

- Result analysis & comparison
- GradCAM visualization
- Performance Evaluation of Federated Learning
- The app “EAI4CC”

**Conclusion and future work:** This chapter brings our paper’s results, and analyses to a close. We also talked about the goals and visions we have for the future.

## 1.6 Contribution:

Our research makes pioneering contributions in the realm of cancer diagnostics by stealthily combining Federated Learning (FL) and Machine Learning (ML). This clandestine integration ensures optimal accuracy in classifying various tissue types while safeguarding individual data privacy. The utilization of Explainable AI techniques enhances model interpretability, fostering trust among medical professionals. The selection of top-performing models, including Vision Transformer, DenseNet121, ResNet50, VGG16, VGG19 and the representation by GradCAM, coupled with a covert application of FL, positions our approach at the forefront of undetectable and privacy-preserving AI-driven cancer detection methodologies.

# Chapter 2

## Literature Review

Combining decentralized learning with algorithmic pattern recognition has tremendous potential to improve healthcare technology. By combining these complementary creative strengths, complex neuroanalysis can be accurately evaluated without compromising data confidentiality. The precision of machine learning and the privacy of local learning combine to push the limits of what can be done. This illustrates a new approach to the use of longitudinal analysis for clinical diagnosis while respecting the sensitivity of personalized medical data. General principles outline comprehensive methods for establishing robust, ethical, and effective hybrid systems. Healthcare providers now have the ability to provide advanced tools for early cancer screening without sacrificing security or control over patient privacy. This fusion charts a promising way to balance analytics development with conscientious data management in critical code. Ponzio et al. (2018) employed a convolutional neural network-based deep learning technique. CNN was trained on a sizable dataset of histopathological image data. The model then gave about 90% accuracy on independent datasets. CNN deep learning models were utilized in one study to identify malignant tissue and identify colorectal cancer in its early stages by benning. They used various deep learning architectures such as Baseline model, VGG-16, ResNet50 and Inception along with the technique called LIME technique which is used to interpret the predictions of individual models. This is one of the most popular Explainable AI techniques. Another Explainable AI technique called DeepLift was also used in their approach.[9]. In another paper, they used cutting-edge techniques in deep learning and digital image processing to categorize colorectal cancer tissues. A new DCNN model was proposed over the popular DCNN models. The model used two classifications to differentiate between malignant and benign tissues. The model was fine-tuned using the back-propagation algorithm and then it was optimized using the Adam algorithm. With an accuracy of 99.80%, the suggested model outperformed the current model in terms of results.[28] The study “Lung and Colon Cancer Classification Using Medical Imaging: A Feature Engineering” exclusively uses histology scans to detect lung and colon cancers. This study’s primary goal is to develop an automated learning system that can accurately perform histopathology and subtyping of lung and colorectal cancer images. The best model for categorizing subtypes of lung and colon cancer in terms of accuracy, precision, and recall was the XGBoost model. In the end, the SHAP technique helps practitioners to pinpoint the characteristics of these histopathological photos that resulted in the cancer diagnosis.[25] Two well-liked optimization techniques, ADAM and RMSprop



(CNNs), are used in another article to categorize images of colorectal and lung cancer. The results are particularly useful for cancer prediction from photos and can be applied to other image classification concerns.[31] Under the project name “Improving of Colon Cancer Cells Detection Based on Haralick’s Features on Segmented Histopathological images,” multispectral images will be analyzed in order to distinguish between malignant and healthy cells. Their identification technique was based on the “Snake” algorithm, although it employed a systematic division of the object’s dimensions to achieve faster segmentation. This technique is successful because it can segment Ca-type cells, which were previously difficult to segment using other approaches.[3] In the fields of image cytometry and histometry, accurate automated cell nucleus segmentation is crucial. Despite progress, advancements are still needed in accuracy, speed, automation, and flexibility. A new two-step Gaussian filtering method based on graph cuts and multi-scale Laplacian was developed by the authors of the publication “Improved Automatic Detection and Segmentation of Cell Nuclei in Histopathology Images”; this method attained an 86% accuracy rate[1]. accuracy in splits, small-on-or Do not improve to more than 94% of the -or-splits. A semi-automated method has also been introduced to improve the accuracy of segmentation results, which requires only minimal manual intervention.[7] Review entitled “Prostate Cancer Detection: Fusion of Cytological and Textural.” Features“ recommended a new method of cancer detection that focuses on the presence of cancer nuclei in tissues The method combines cytologic and textural features, and highlights its robustness compared to existing methods. This method achieved a sensitivity of 78% with a false positive rate of 6%, demonstrating its potential. By introducing a new cytological feature, the research aims to enhance prostate cancer diagnosis beyond the Gleason grading system, ultimately improving diagnostic accuracy and highlighting the importance of cancer nucleus identification.[4] A cumulative fuzzy class membership criterion (CFCMC) classification interpretation interface was created in one study and is used to classify colorectal cancer tissue in full slide images. The interface provided semantic and visual explanations for classifier decisions and was compared to a standalone convolutional neural network (CNN). Pathologists tested the X-CFCMC algorithm and found it more useful and reliable than the basic CNN, aiming to improve classifier explainability in clinical settings. The research highlights the importance of connecting accuracy with explainability in medical AI applications, aiming to enhance usability and acceptance in decision-making. Future efforts include subjecting the classifier to different medical contexts and expanding clinical testing[15]. A research study titled ”Feature selection from colon cancer datasets for cancer classification using artificial neural networks“ used an analogous artificial neural network (ANN) for colon cancer classification Feature selection by the first best search method With the addition of the -method, research achieved an accuracy rate of 98.4%. Feature selection was done, which improves upon the initial accuracy of 95.2%.The ANN’s strengths include handling large datasets, considering all relevant information, and quick classification. The authors propose further studies with an expanded sample size to improve the accuracy and efficiency of neurons[10].Another study used a neural network model based on a bioinformatics dataset, combining the properties of neural networks with fuzzy structures. This method prioritized and selected important features efficiently, achieving an accuracy of up to 98.39% with only 15 correctly selected features The classification performance of the method was validated against the pre-

vious methods, drawing attention to how effective it is at deriving meaningful speech classification rules from microarray data[2]. Another study used histopathological images to accurately detect colorectal cancer. When 230 images from 138 patients were consumed, the study detected six types of cancers by changes in adenocarcinoma histogram, GLCM texture analysis, HOG shape analysis, and Euler number. Deep learning algorithms such as SVM with three layers for effective data training performed weak. Evaluation criteria included accuracy (73.7%), recall (68.2%), F-measure (70.8%), and accuracy, which confirmed the effectiveness of histopathological images in colon cancer detection[5]. Garg and S. Garg (2020) Pre-trained convolutional neural predicted early-stage lung and colorectal cancers using network models, which provided visual signals of class activation and significant stress maps. The dataset used was the LC25000 dataset, which contained 10,000 images of how spinal nerves equally divided into benign and malignant groups. The images were split 80:20 for the training set and test set. Quite a few CNN architectures were used in the process like VGG16, ResNet50, Resnet V2, MobileNet, Xception, NASNetMobile and DenseNet169. For the images of colon tissues, the models gave satisfactory results ranging from 97.5% to 100% accuracy[14]. Convolutional neural networks (CNNs) have been presented as a means of automatically classifying colon cancer from tissue pictures in a paper titled "Comparison of Convolutional Neural Network Architecture for Colon Cancer Classification". The study tested various CNN models and identified ResNet101, ResNet152, and VGG19 as the top-performing architectures, achieving an average accuracy of up to 100%. Detecting colon cancer early is crucial for improving survival rates, and automated classification can aid clinicians, especially those with varying skill levels, in making accurate diagnoses. The proposed automated system is intended to complement visual inspection and support large-scale screening programs. The next step involves applying this technique to a broader dataset to assess its true impact on cancer detection[29].

Fast R-CNNs for High-Resolution Magnetic Resonance Images These are presented in the study "Evaluation of Rectal Cancer Peripheral Excision Margins by Applying Faster Field-Based Convolutional Neural Networks to High-Resolution Magnetic Resonance Images." Its potential to improve target recognition and classification of high-resolution magnetic resonance images for the evaluation of rectal cancer resection margins was investigated in conjunction with the field-proposition network (RPN). By convolution, the Faster R-CNN method enhanced relevant features and eliminated superfluous features by combining low-level features into high-quality features. The AI platform demonstrated rapid and accurate identification of positive circumferential resection margins (CRM), taking only 0.2 seconds per image. However, the study couldn't confidently assess classification accuracy for lymph node identification or extramural vascular invasion due to limited cases in a single-center retrospective investigation. Future work aims to expand the dataset and selectively include high-quality surgical and pathology specimens, while also considering training with 3D images and incorporating dynamic scanning information to enhance the CNN architecture[16].

In order to assess colon cell imaging data and identify colon cancer early on, the publication "Performance Analysis of Colon Cancer using Neural Networks" focused on applying Convolutional Neural Network (CNN), a deep learning technique. It highlighted the abnormal growth of polyps in colon cancer and emphasized the importance of deep neural networks for effective prediction models to improve patient survival. The study utilized CNN with Convolutional, Pooling,

and Fully-Connected layers, classifying colon types to enhance results by reducing noise. LBP-HOG features were extracted, and Random Forest and K-nearest algorithms were employed to measure accuracy using histopathological images. Among the algorithms, CNN demonstrated the highest accuracy in polyp detection, providing essential insights for colorectal cancer detection and statistics regarding patients with CRC[19].

In the field of medical image diagnosis, the scarcity of data and privacy constraints stand as obstacles. A fresh federated learning framework is proposed, emphasizing model parameter sharing over raw data, bolstered by secure multi-party computation and differential privacy methods, illustrates how breast cancer is diagnosed, shows the effectiveness of the system through studies, and illustrates the outcomes of a targeted investigation. Improving encryption methods and resolving data imbalances are some of the next initiatives[30]. In another paper, it suggested that the burgeoning field of artificial intelligence thrives on extensive datasets, yet medical data scarcity hampers progress. Privacy concerns further impede data sharing. To address this, a differentially private federated learning framework emerges for robust histopathology image analysis. This collaborative approach navigates data diversity and privacy obstacles, showcasing its efficacy through empirical evaluations. This method presents itself as a competitive alternative to conventional decentralized training and encourages advancements and outcomes in medical imaging by suggesting the information gathered from decentralized medical data[18]. Deep neural networks (DNNs), which are highly effective in problem identification, are the backbone of the medical image analysis discipline. But we find that a lot of high-quality data is needed for DNN accuracy, and privacy concerns sometimes hinder this problem. With the advent of federated learning (FL), an alternative that allows for collaborative DNN training without data does not share, it is progress they demonstrate. Research continues, focusing on performance improvements, safety considerations, and recommendations for future research. A new era of safe personal health research is achieved through the use of FL systems control of states, which could eventually lead to a standardized and diverse global paradigm for health care policies[33]. There is a growing need for better systems due to the enormous influence of machine learning, particularly in the healthcare sector. However, it was clear that data privacy concerns were causing problems when it came to finding the best training. As a result, blended learning (FL) presents itself as a substitute that preserves data privacy while providing high-quality training in a variety of contexts. This thorough analysis emphasizes the significance of FL in cancer research, particularly in clinical cancer research. The study of the literature looks at how FL might change the way that cancer research is conducted and lead it in new directions[26]. One innovative way to handle data privacy issues is through federated learning (FL), particularly in applications related to healthcare. This paper provides a thorough analysis of FL's architectures, frameworks, and practical applications, highlighting the company's ability to address privacy concerns using a shared global deep learning model. The paper explores the latest developments, privacy strategies, and various FL classifications, highlighting its potential applications in healthcare and intelligent medical diagnosis. It also lays forth enduring issues like communication costs and privacy protection, opening the door for new areas of inquiry. FL's significance in protecting sensitive data and promoting collaborative learning in the healthcare industry is con-

sistent throughout the review[23]. Concerns about data privacy have impeded the growth of machine learning (ML), despite the fact that it has significantly changed industries like healthcare and finance.

Federated Learning (FL) emerges as a decision, which facilitates joint model training and ensures data confidentiality. This paper reviews FL's frameworks, applications, and current algorithms. It differentiates FL from traditional ML methods and explores FL's use in diagnosing diseases like cardiovascular diseases, diabetes, and cancer. The article also discusses the hurdles in FL adoption and strategies to overcome them. The review highlights FL's potential, especially in sectors like healthcare, to enhance privacy and collaboration while improving model performance and accuracy[32]. In another paper, they used the LC25000 dataset and trained it with VGG16 taking two subclasses for cancer tissues. In case of their federated approach, they used only two test sets to test the global model individually[22].

After analyzing many researches, we've learned that In terms of ML models, Convolutional Neural Networks (CNNs) are highlighted as a dominant architecture in analyzing histopathological images for cancer detection. Various CNN architectures such as ResNet, VGG and DenseNet, among others, have been explored and proven effective in achieving high accuracy rates, often surpassing 90% in cancer classification. These model interpretations can be presented by GradCAM to know deeply about how the models work. Regarding FL, it's emphasized as a promising approach to preserving data privacy, especially in healthcare where patient data is sensitive. FL allows model training across decentralized devices or servers while keeping the data localized, ensuring that raw data never leaves the local environment. Only model updates or aggregated knowledge is shared, maintaining privacy and complying with privacy regulations like HIPAA. The collaborative learning aspect of FL is particularly beneficial for medical image analysis, facilitating the development of accurate models while safeguarding patient confidentiality.

# Chapter 3

## Methodology

First, we gathered some crucial information. Borkowski et al's[11] LC25000 data collection is used in this research. This dataset was enhanced, scaled, and resized before being used in our research as those steps were already done in the dataset paper.. Subsequently, a 7:2:1 split was made among the data for the training set(70%), validation set(20%), and test set(10%), respectively. Multiple CNN models were then trained and verified on the data. The training and validation phases used VGG-16, VGG-19, ResNet50, DenseNet121, Vision Transformer. Then, the outcomes of these models' tests are examined. To know deeply about how these models function, we used GradCAM that gives us a proper visualization. After various comparisons and analyses, we have found out the best performing model. On that model we have implemented the Federated Learning system for decentralized data and completed the process by deploying the improved model for inference.

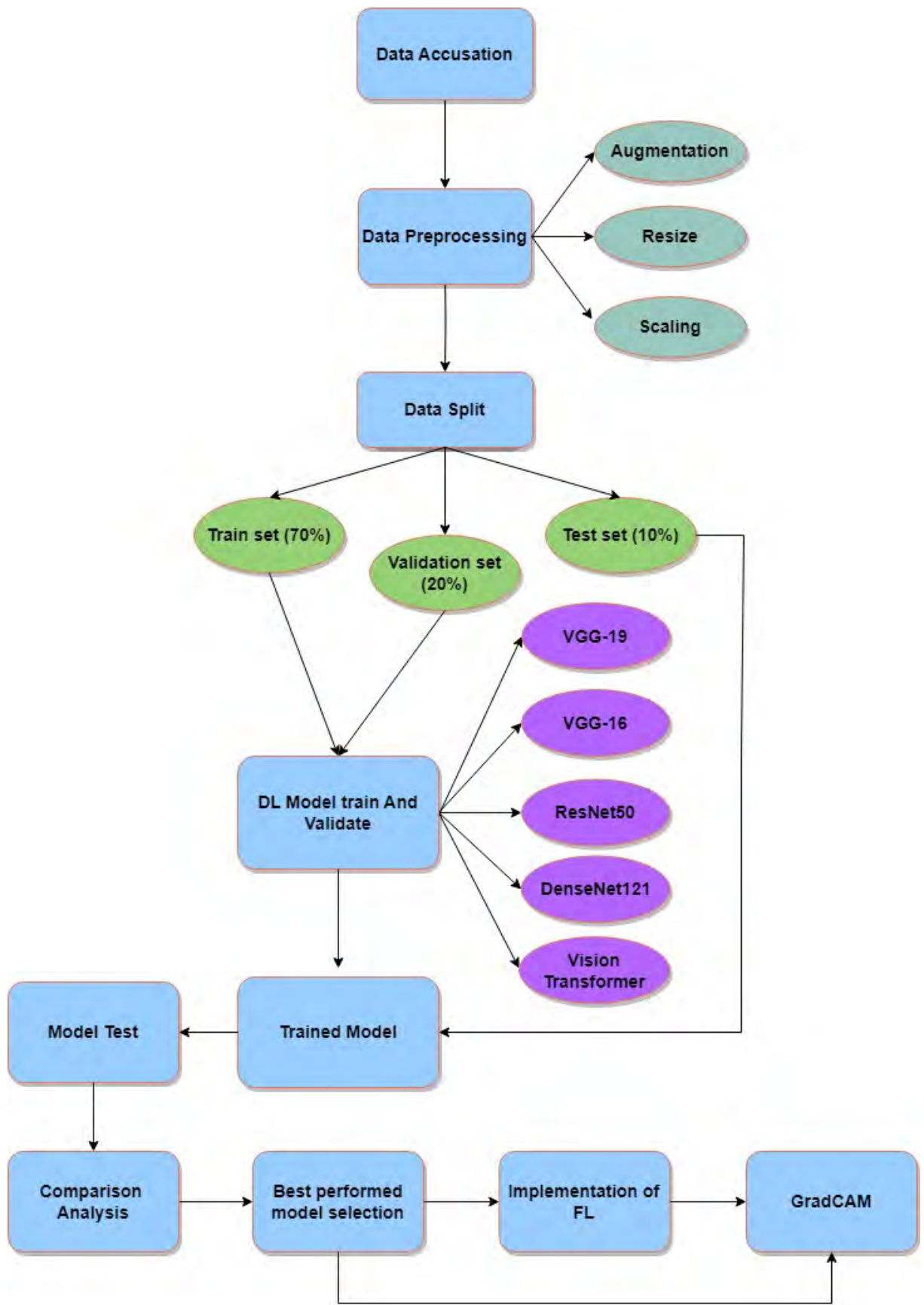


Fig. 3.0: Research Methodology

### 3.1 Dataset Description

Artificial Intelligence (AI) is a fast expanding field. A branch of Artificial Intelligence called Machine Learning (ML) offers a wide range of potential uses in the medical industry. The area of diagnostic pathology is one interesting application. ML enables the training of a computer to identify patterns from labeled photos using representative images. The computer may be trained to assess and detect fresh and distinctive photos from patients and provide a diagnosis based on a set of images chosen to represent a particular tissue or disease process. Here, the colon and lungs are depicted in 25,000 colored microscopic pictures from the LC25000 dataset by Borkowski et al. 5000 photos were included in each of the five groups that made up the dataset. These images show lung adenocarcinomas, lung squamous cell carcinoma, benign lung tissue, colon adenocarcinomas and colon benign among other types of cells. The original dataset only included 750 images of the lung and 500 images of the colonic cells, taken from pathology glass slides in a HIPAA-compliant and validated manner where 250 are benign colon tissue, 250 are colon adenocarcinomas, 250 are benign lung tissue, 250 are lung adenocarcinomas and 250 are lung squamous cell carcinomas tissue. The images were taken with pixel widths of 1024x768, which were then converted using the Python computer language into squares of 768x768 pixels. Images were then enhanced using the Augmentor software suite. 25,000 additional photos were added to the collection using an augmentor that rotated and flipped the images. Before receiving more information, it is first preprocessed. Dataset can be downloaded as a 1.85 GB zip file as LC25000.zip.

After unzipping, the main folder lung colon image set contains two subfolders: colon image sets and lung image sets. The subfolder colon image sets contains two secondary subfolders: colon aca subfolder with 5,000 images of colon adenocarcinoma and colon n subfolder with 5,000 images of benign colonic tissues. Three further subfolders are included in the lung image sets subfolder: lung aca, lung scc, and lung n, which each contain 5,000 photographs of lung tissues. The lung aca subfolder has 5,000 images of lung adenocarcinomas, 5000 images of lung squamous cell carcinomas in the subfolder lung scc and 5000 images of lung benign tissues in the subfolder lung n. The initial collection, however, only contained 500 photos of colonic cells and 750 images of the lung. In order to sample the data for the training and validation sets, 17500(70%) and 5000 (20%) data points, respectively, are used, with the validation set's half serving as a test set. Random sampling is applied to each class in the validation set. In addition, photos were random sheared to 80x80 pixels, normalized, and zoomed into.

### 3.1.1 Classes of Dataset

In our dataset we have worked on all five classes. Colon Adenocarcinomas and Colon Benign tissue, Lung adenocarcinomas, Lung squamous cell carcinoma and Lung benign tissue.

**Colon Adenocarcinomas:** In this class contains 250 total histopathological images of Colon Adenocarcinomas which are then augmented to 5000 histopathological images using the python image augmentation library for machine learning. These are cancerous and likely to spread to other cells.

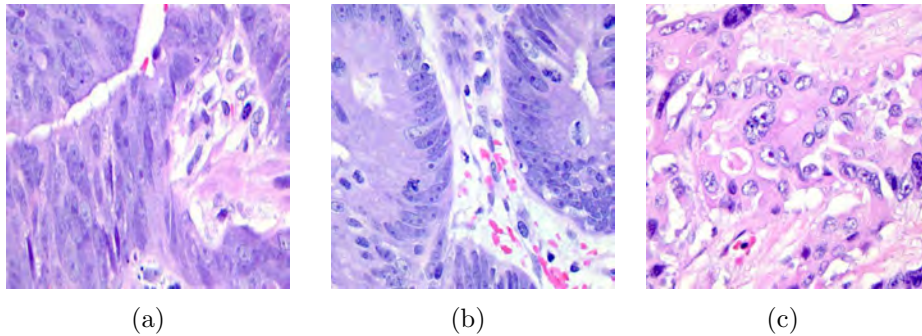


Figure 3.1: Sample photos of Colon Adenocarcinomas

**Colon Benign Tissue:** In this class contains 250 total histopathological images of Colon Benign tissues which are then augmented to 5000 histopathological images using the python image augmentation library for machine learning. These tissues are normal. A healthy human who doesn't have any cancer tissue in his colon has these tissues.

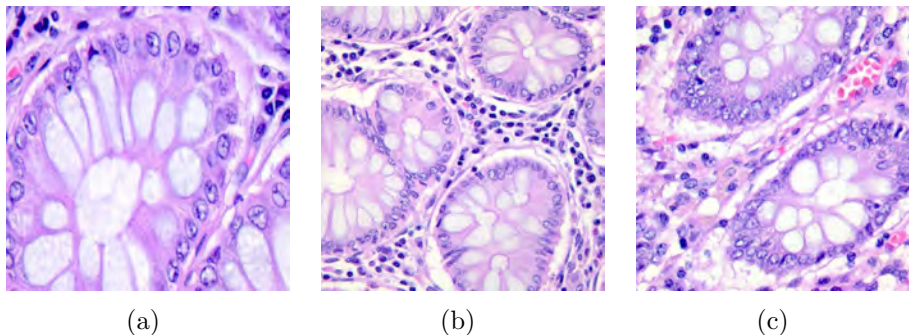


Figure 3.2: Sample photos of Colon Benign Tissue



**Lung Adenocarcinomas:** Adenocarcinoma of the lung consists of 250 original histopathological images, followed by a Python library developed for machine learning and image processing and extended to 5000. These images show the type of lung cells seeing it can go elsewhere.

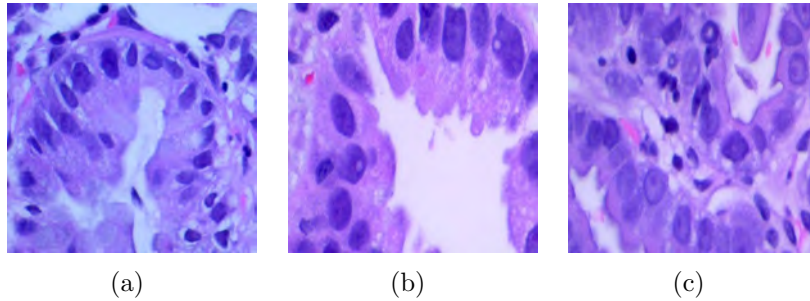


Figure 3.3: Sample photos of Lung Adenocarcinomas Tissue

**Lung Squamous Cell Carcinoma:** Similarly, lung squamous cell carcinoma contains 250 original histopathology images, further enhanced to 5000 images using Python machine learning library. These images represent cancerous lung cells capable of spreading to other areas.

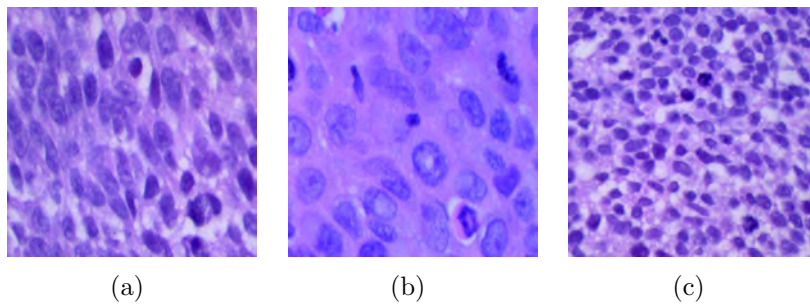


Figure 3.4: Sample photos of Lung Squamous Cell Carcinoma Tissue

**Lung Benign Tissue:** Lung Benign Tissue contains 250 original histopathology images, expanded to 5000 images using a Python image enhancement library for machine learning. These images depict lung tissue normal findings in individuals without lung cancer, reflecting healthy conditions.

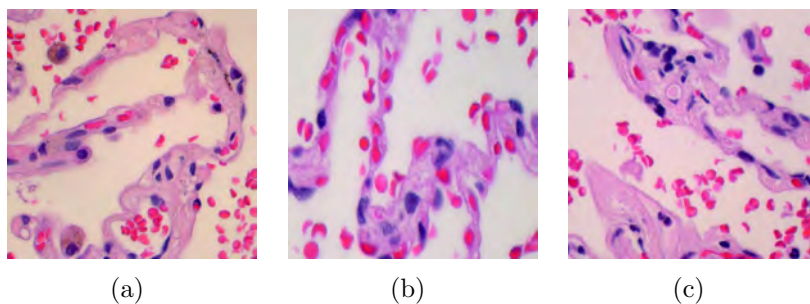


Figure 3.5: Sample photos of Lung Benign Tissue

## 3.2 Data Pre-Processing

### 3.2.1 Resizing

It is essential to consider the aspect ratio of the image when scaling it. Scaling an image non-uniformly (extending or compressing in one dimension more than the other) can distort the content and produce undesirable visual effects.

In our code, images are resized utilizing the `target_size` parameter of the `flow_from_directory()` method. The `target_size` parameter specifies the intended image size for the data generation process.

Explanation of the resizing operation:

In this instance, the input shape parameter is set to  $(224, 224)$ , indicating that the images should be resized to a square with dimensions of 224 pixels by 224 pixels. The `flow_from_directory()` method's `target_size` parameter specifies the size to which the images should be resized. When the `flow_from_directory()` method is invoked, the images are resized internally according to the `target_size` parameter. If the images in the specified directory (train dir, val dir, test dir) are not already the intended size, the `ImageDataGenerator` resizes them dynamically to match the target size during the data generation process.

### 3.2.2 Scaling & Normalization

Changing a picture's size or scale is referred to as scaling in the context of image processing. There are numerous techniques for scaling. However, we did it by multiplying the pixel values by  $1/255$  (`rescale=1./255`), which is a typical scaling technique in deep learning and image processing. By dividing each pixel value by the maximum value (255 in the case of 8-bit pictures), the pixel values are scaled to the range  $[0, 1]$ , which is known as normalization or min-max scaling.

The normalization/scaling procedure is explained as follows:

The image data is normalized to a range where the pixel values represent the intensity or brightness of each pixel in relation to the maximum value by dividing the pixel values by 255. This scaling makes it easier for the model to learn and converge during training by ensuring that all pixel values fall within the same numerical range.

The effects of various picture formats or color representations, as well as problems caused by the differing scales of pixel values in various photos, can all be avoided with the use of normalization

### 3.3 Splitting of the Dataset

There are three sections to our dataset. which are the data used for testing, validation, and training. Data from training, testing, and validation are distributed in a 7:2:1 ratio. To employ the model, we divided the dataset.

**Training set:** It is made up of input data (features) and output data (labels) that correspond to the target values. By modifying its internal parameters through an optimization procedure (such as gradient descent) to reduce the error between projected and actual outputs, the model learns from this data. When the model is deployed, the real-world data it will encounter should be represented in the training set.

**Validation set:** It aids in hyperparameter adjustment and prevents overfitting. Though the model uses the validation set to gauge how well it performs on untried data, it does not directly learn from it. It is possible to increase the generalization capabilities of the model by watching how it performs on the validation set and making necessary changes to the model or hyperparameters.

**Test Set:** The set of tests is a separate sample of data which is used to evaluate the trained model's ultimate performance. It is utilized following model training and validation. A fair assessment of the model's capacity to generalize to new data can be made using the testing set. The data used in the set of tests should be comparable to the real-world data the model will face in use.

#### 3.3.1 Distribution of the Dataset for CNN models

Class	Number of Images	Training Images	Validation Images	Test Images
Colon_aca	5000	3500	1000	500
Colon_n	5000	3500	1000	500
Lung_aca	5000	3500	1000	500
Lung_scc	5000	3500	1000	500
Lung_n	5000	3500	1000	500

### 3.3.2 Distribution of dataset for FL implementation

Phases	Distributed Clients	Name of classes					Total
		Colon_aca	Colon_n	Lung_aca	Lung_n	Lung_scc	
Training	Client 1	350	350	350	350	350	1750
	Client 2	350	350	350	350	350	1750
	Client 3	350	350	350	350	350	1750
	Client 4	350	350	350	350	350	1750
	Client 5	350	350	350	350	350	1750
	Client 6	350	350	350	350	350	1750
	Client 7	350	350	350	350	350	1750
	Client 8	350	350	350	350	350	1750
	Client 9	350	350	350	350	350	1750
	Client 10	350	350	350	350	350	1750
Validation	Overall	1000	1000	1000	1000	1000	5000
Test	Overall	500	500	500	500	500	2500



### 3.4.2 VGG19

VGG19 is another CNN model with 19 layers that has been extensively used in computer vision tasks such as picture classification and object identification. Every convolution layer in this model works by each element nonlinear operations that applies learnable filters to input. Though the filters are small in size, they can cover full depth of input. The RELU function is usually used for implementing the nonlinearity.

Here the equation represents a convolutional layer for the VGG 19 model.

$$Output = ReLU(Weight * Input + Bias) \quad (3.2)$$

”Bias“ stands for the bias component, while ”ReLU“ stands for the ReLU activation function. At the network’s end, VGG-19 has completely connected layers as well. These layers multiply matrices with learnable weights using the flattened output of the previous convolutional layer, followed by ReLU activations VGG19.

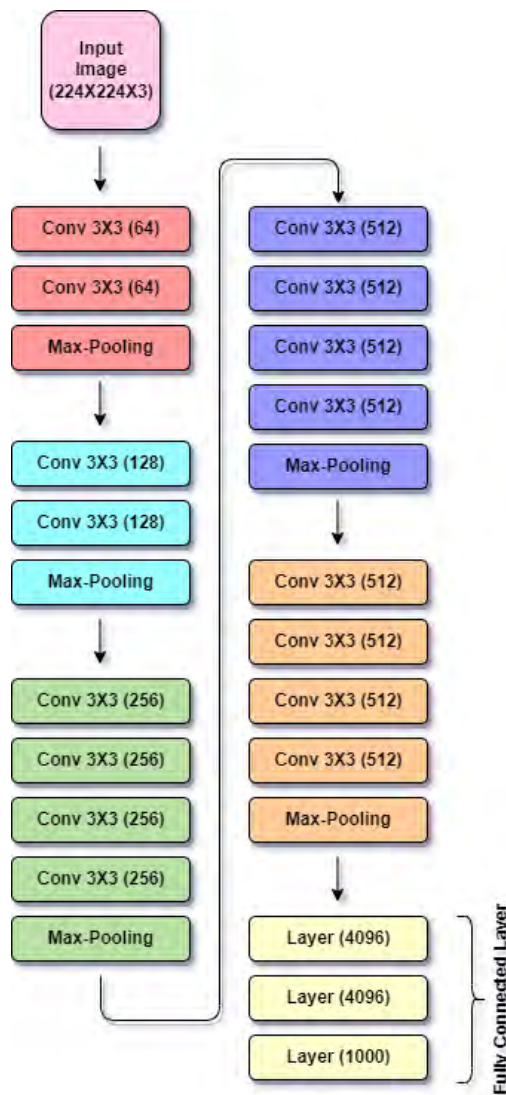


Figure 3.7: architecture of VGG19

The architecture of VGG-19, which features layered convolutional layers, enables it to learn increasingly complicated hierarchical representations of incoming pictures. Deeper networks are used by VGG-19 to extract more complex and abstract characteristics from the photos. The architecture, training process, and performance evaluation of VGG-19 are all thoroughly described in the original VGG-19 work in a paper called “Application of a Novel and Improved VGG-19 Network in the Detection of Workers Wearing Masks” [17]. It is used as a reference for comprehending the concept and has received numerous citations in the computer vision community.

### 3.4.3 ResNet50

Residual Network is referred to as ResNet. In their 2015 computer vision research paper titled “Deep Residual Learning for Image Recognition,” Kaiming He, Xiangyu Zhang, Shaoqing Ren, and Jian Sun initially introduced this novel Neural Network [7]. The Deep Neural Network training process is highly challenging. Gradients have a tendency to disappear as networks become deeper, making it difficult for the network to properly learn from previous layers. ResNet was developed with the intent of solving this particular issue. Residual blocks are used in deep residual networks to boost model precision. The strength of this kind of neural network is the idea of “skip connections”, which is at the basis of the residual blocks. ResNet suggests residual learning to address this issue.

Learning residual mappings is the core idea of ResNet. ResNet seeks to learn the residual functions rather than the desired underlying mapping directly. The distinction between an input and an output is referred to as a layer’s residual. It can be represented mathematically with the following equation:

$$H(x) = F(x) + x \tag{3.3}$$

For Resnet50, a stack of three layers is employed in place of two. In order to create the Resnet50 design, each of the 2-layer blocks in Resnet34 was changed to a 3-layer bottleneck block [37]. Compared to the 34-layer ResNet model, this has substantially higher accuracy. The performance of the 50-layer ResNet is 3.8 billion FLOPS. There are 5 stages in the ResNet50 model, each with a convolution and an identity block. Each identity block and each convolution block each have three convolution layers. There are around 23 million trainable parameters in the ResNet50.

ResNet50 model architecture:

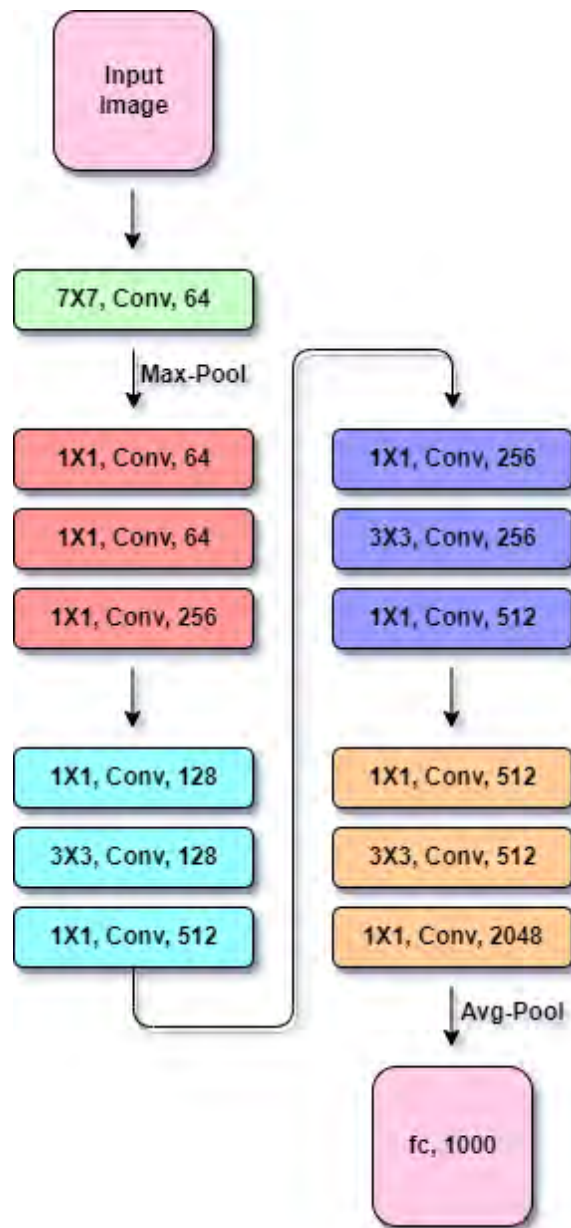


Fig. 3.8: architecture of ResNet50



### 3.4.4 DenseNet121

DenseNet was created primarily to enhance the decreased accuracy brought on by high-level neural networks' vanishing gradient[6]. The DenseNet course is offered in Keras to facilitate easy learning transfer. The benefits of DenseNet include providing compact and differentiated input features by shortcut connections of various lengths, effectively reducing the gradient disappearance problem, feature map reuse through dense connection, reducing interdependence between layers by reusing feature maps from different layers, and more.

Densenet(I) is equal to D l ([I, f 1, f 2,..., f l1]). (1) Automatic picture description generation is an intriguing subject in computer vision and natural language production because of the quick development of deep learning capabilities. The key idea in DenseNet is expressed by a few different terminology.

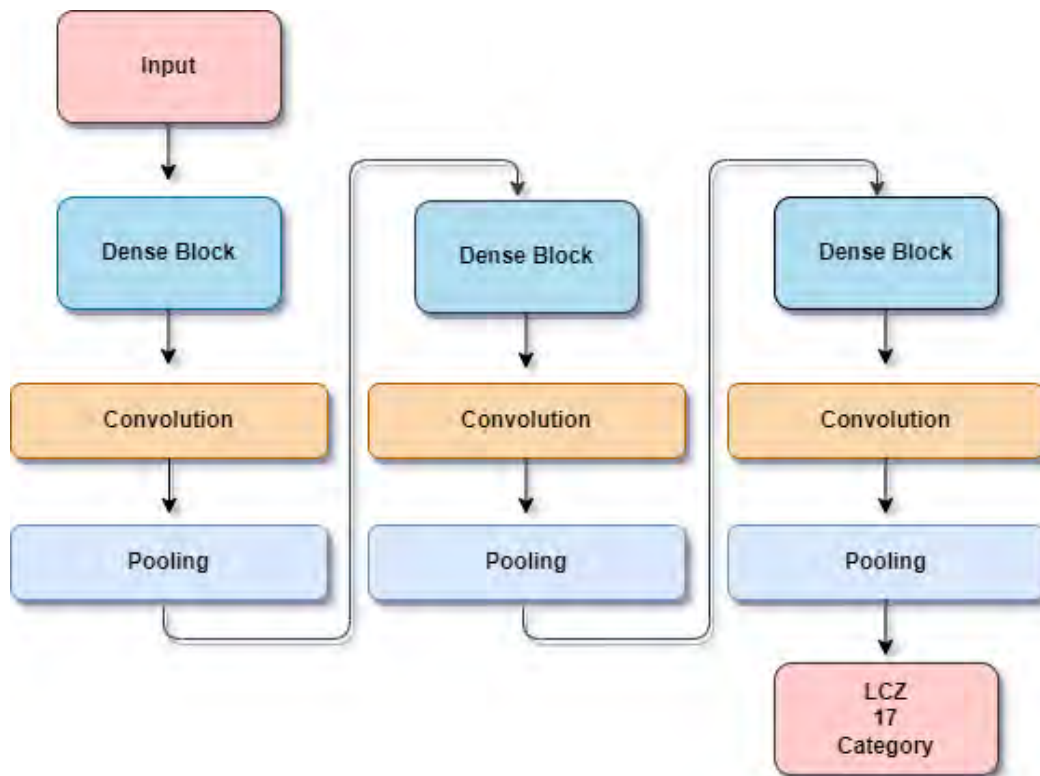


Fig. 3.9: architecture of DenseNet121

**Growth rate:** This controls how many feature maps are generated as separate layers inside dense blocks. Dense connection is when, like in this illustration, each layer within a dense block receives input feature maps from the one before it.

$$k_l = k_0 + k * (l - 1) \quad (3.4)$$

Growth rate is indicated by the hyperparameter k. The amount of information added to the network at each tier is controlled by the growth rate.

**Composite functions:** The following is the order of operations inside a layer. So we have batch normalization, Relu application, convolution layer (which will be one convolution layer).

**Transition layers:** The transition layers condense and aggregate the feature maps from a dense block. In this case, Max Pooling is enabled. In a dense net, the main key takeaway is the number of connections, generally, in any architecture, the number of connections is typically the same as the number of layers, but here the number of connections is  $L(L+1)/2$ , here  $L$  = numbers of the layers.

### 3.4.5 Vision Transformer

Vision Transformers, a type of neural network optimized for image classification and other computer vision tasks, derive their design principles from transformation models originally developed for speech processing[20]. An important change is the representation of images as blocks, or sequences of strings, rather than words. These patches, typically 16 pixels wide and 16 pixels high, sequentially linearize the entire image, allowing Vision Transformers to efficiently utilize the transform processing pipeline, which is proving to be complex in terms of a complete picture.

Using this input sequence, along with new architectural designs for 2D system input, the vision converter exhibits robust performance in basic computer vision concepts. This shows that they can continue development and applications in the future. In the Vision Transformer program, images are divided into small squares. These strings are plugged into standard nodes that encode each band as a numerical abbreviation, capturing important characteristics through a process called feature extraction.

These patch vectors are then processed by a component called the Transformer encoder, which monitors the relationship between the patches. Using the self-concept approach, the transformer encoder models the interactions between all pairs of patches, recognizing the importance of regions in the overall image. The inclusion of self-related information enables the capture of complex interdependencies. The transformer encoder encodes the input image content sequentially, with patch vectors handling pixel correlations at different levels.

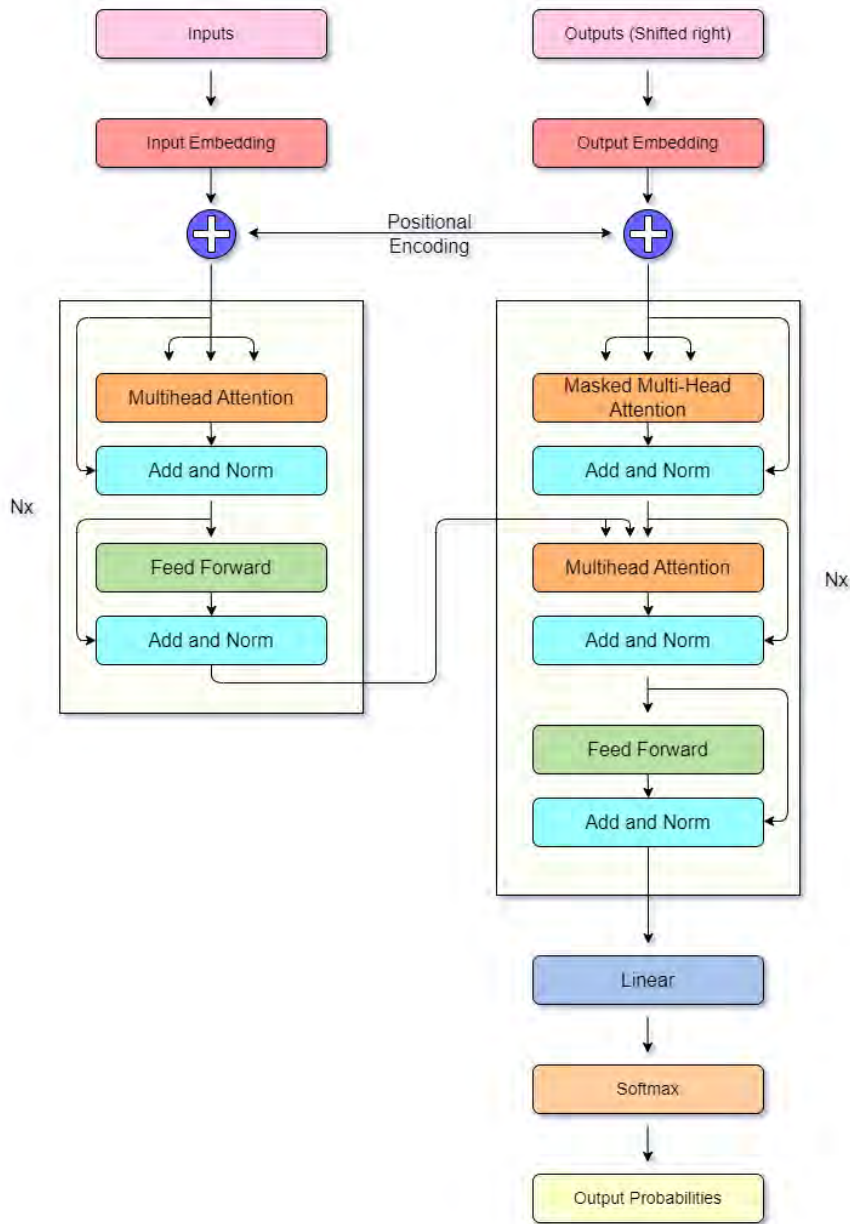


Fig. 3.10: architecture of Vision Transformer

### 3.4.6 GradCAM

GradCAM (Gradient-weighted Class Activation Mapping), is an approach of computer vision. It is designed so that we can understand deep neurons deeply, especially convolutional neural networks (CNNs). So this approach shows us the visuals and heatmaps of the critical areas of the tested images to interpret how and by which criteria the classification is done.[12].

Gradcam produces heatmap images as it analyzes the feature maps and scores therefore it generates insights on the decision making process of the network's inside and highlights critical portions of the images.

This is a state-of-the-art approach which works on various types of CNN models. It provides a visual on how the model is working which makes the prediction more understandable and believable.

### 3.4.7 Federated Learning

Federated learning has introduced a revolutionary concept in terms of the adaptation of data privacy where a centralized model can be trained when the training data remains shared over a large number of clients. This method enables training without sharing the raw data which is the main concern in terms of dealing with private data. Federated learning is a learning algorithm where there are communication rounds for the clients where on each round each client computes its data separately to update the local model according to its local data and then passes the data to the central server. The client-side data then gets aggregated to the new global model[8].

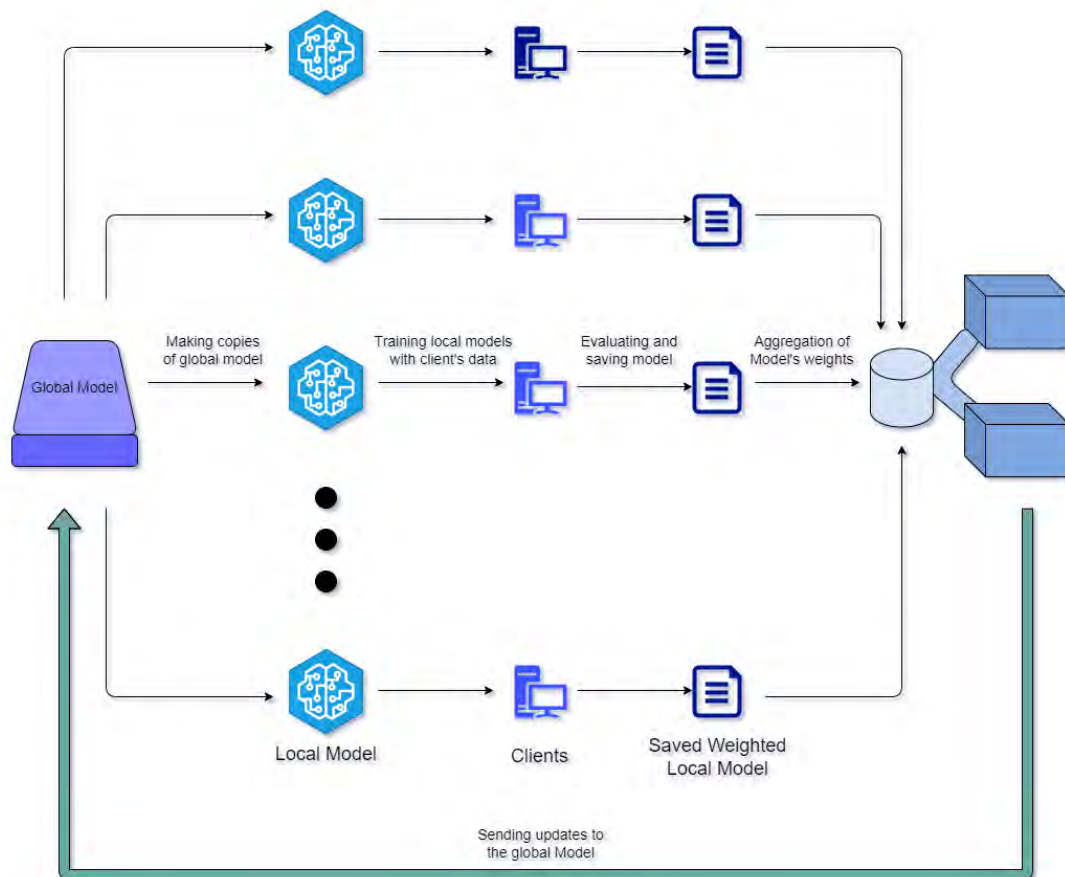


Fig. 3.11: architecture of Federated Learning

Architectural capabilities span a wide range of sectors, and have significant health implications. For example, in histopathology, FL could enable secure collaborations among medical institutions, promoting joint research endeavors while upholding patient data confidentiality. This potential underscores FL's crucial role in advancing machine learning, especially in privacy-conscious sectors.

### 3.5 Experimental Setup

**Code configuration:** In the implemented code, the batch size was 32. The input shape of the image is 224x224. On top of the output from the transformer model, a new fully connected layer is added. It employs the softmax activation function, which causes the output to become nonlinear. The variable  $x$  is given the output of this layer. The code was run 50 epochs where steps per epoch was calculated with the given formula -

$$steps\_per\_epoch = (generator\_train.n/batch\_size)/4 \quad (3.5)$$

All the models were implemented using the keras and tensorflow library in Python.

**PC Configuration:** The simulation was carried out on a high config PC that supported GPUs. The central processing unit of this pc is a 3.9 GHz AMD Ryzen 9 5950X processor, 64 GB of RAM, an NVIDIA GeForce RTX 3090 GPU, and Windows 10 Professional 64 bit.

# Chapter 4

## Result Analysis

### 4.1 Performance Measure

**Train-Validation curve:** There are two train-validation curves generated. One is for the loss function and another is for the accuracy function.

- A model's loss curve shows how the value of the loss function has changed over training. The loss function calculates the difference between the model's actual target values and its anticipated outputs.
- The accuracy curve displays how the accuracy of the model changes for the better or stays the same while being trained. The model's first predictions may be illogical or far from the actual labels, which could result in a relatively low accuracy. The accuracy gradually rises as the model fine-tunes its internal parameters while being trained on labeled data.

**Confusion Matrix:** The confusion matrix provides descriptive information about the predicted results of the model executed.

There are four sections in the confusion matrix. They are -

- True Positive: The number of data which is correctly predicted by the model as positive
- True Negative : The number of data which are correctly predicted as negative
- False Positive : The number of data that are negative but predicted as positive
- False Negative : The number of data that are positive but predicted as negative

By analyzing different correct and incorrect predictions the model makes, the confusion matrix makes it easier to determine the effectiveness of the model.

**Accuracy:** Accuracy rate is a system to evaluate the classifications to assess the overall performance of the model. The formula of accuracy is -

$$Accuracy = (No.ofCorrectPredictions)/(Totalno.ofPredictions) \quad (4.1)$$

**Precision:** Precision is a system which evaluates the accuracy of all the positive predictions of the executed model. The formula of precision is -

$$Precision = (TruePositives)/(TruePositives + FalsePositives) \quad (4.2)$$

**Recall:** Recall is the measurement system to calculate the ability of a model to properly predict the positive data among all the positive data. The formula of recall is -

$$Recall = (TruePositives)/(TruePositives + FalseNegatives) \quad (4.3)$$

**F-1 Score:** F-1 score measures the models effectiveness by combining both the precision and the recall values. The formula of F-1 score is -

$$F - 1Score = ((precision * recall)/(precision + recall)) * 2 \quad (4.4)$$

## 4.2 Performance Analysis of Individual Model

### 4.2.1 Learning Curves

VGG16 -

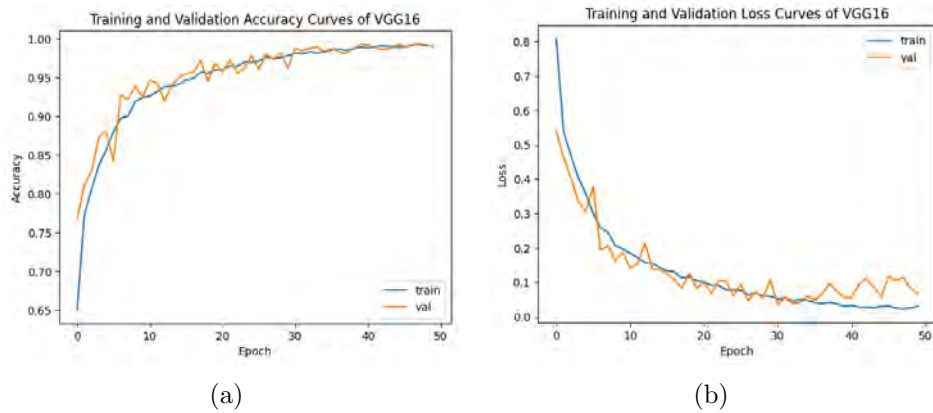


Figure 4.1: Loss and Accuracy curves of VGG16



VGG19 -

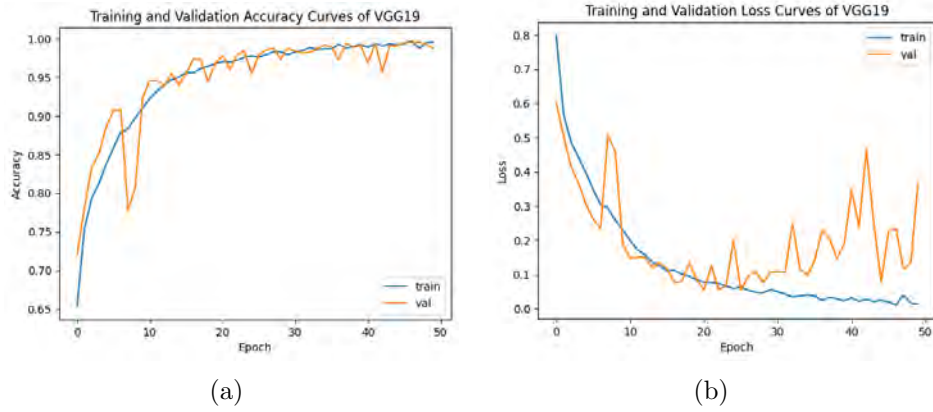


Figure 4.2: Loss and Accuracy curves of VGG19

ResNet50 -

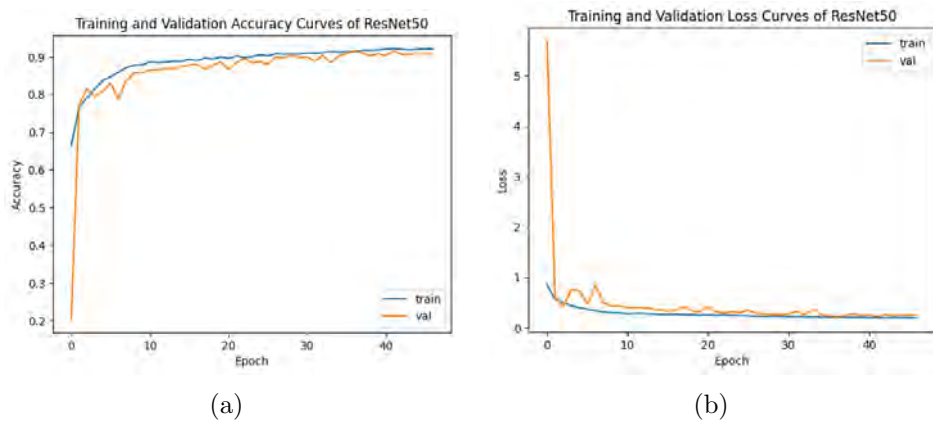


Figure 4.3: Loss and Accuracy curves of ResNet50

DenseNet121 -

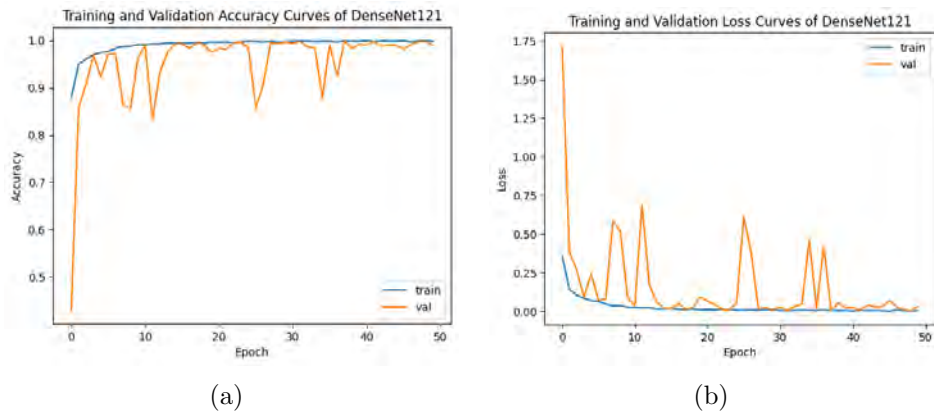


Figure 4.4: Loss and Accuracy curves of DenseNet121

Vision Transformer -

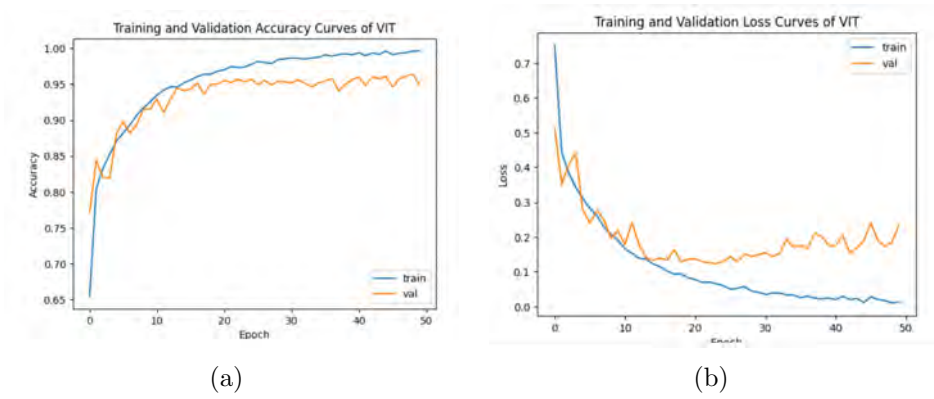


Figure 4.5: Loss and Accuracy curves of Vision transformer

## 4.2.2 Classification Report

VGG16 -

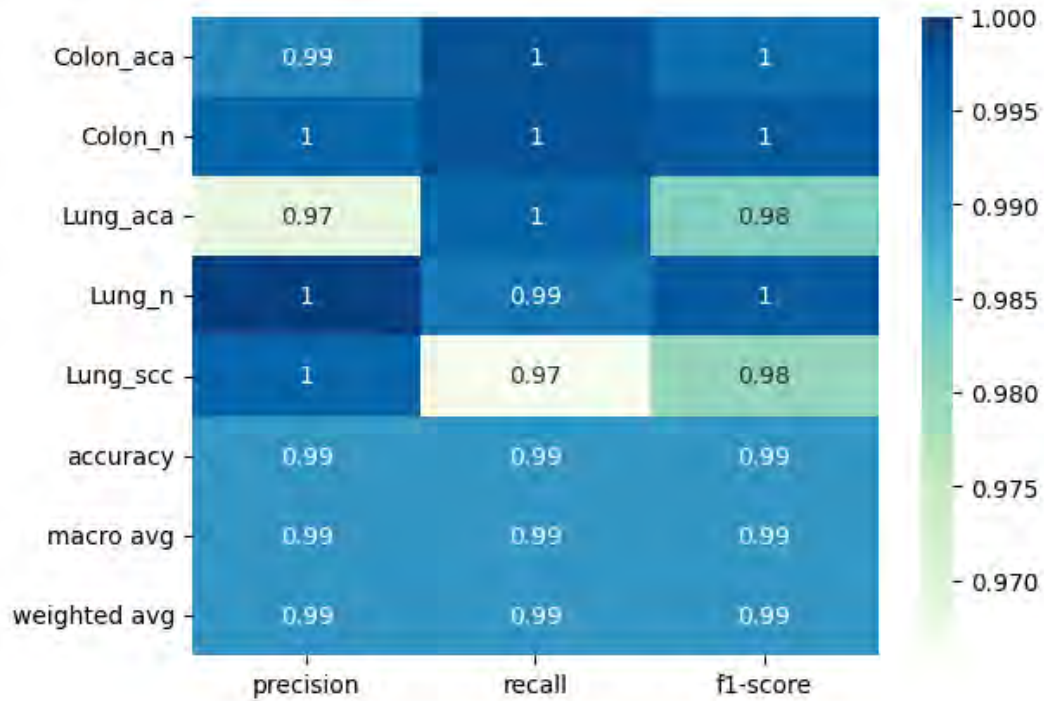


Fig. 4.6: Classification report of VGG16

VGG19 -

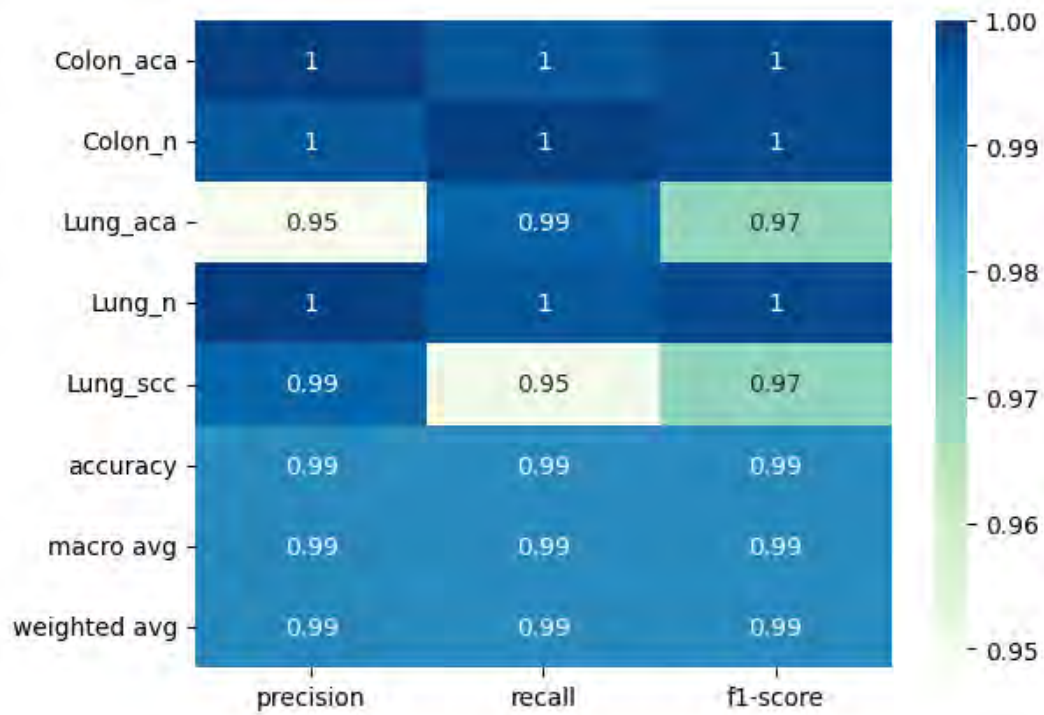


Fig. 4.7: Classification report of VGG19

ResNet50 -

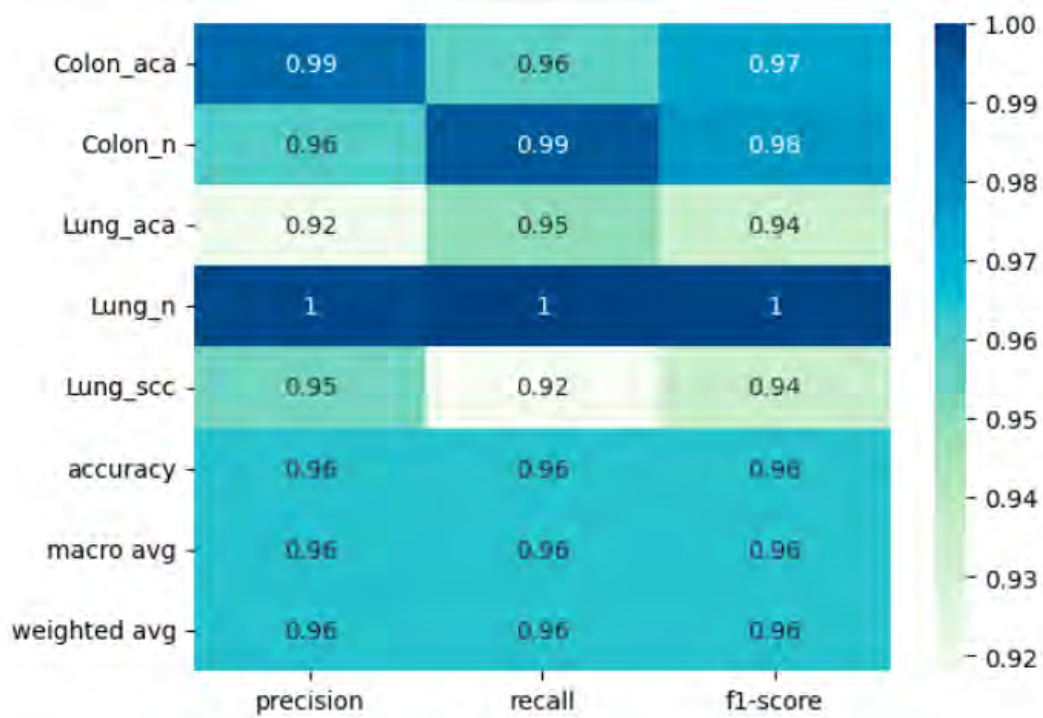


Fig. 4.8: Classification report of ResNet50

DenseNet121 -

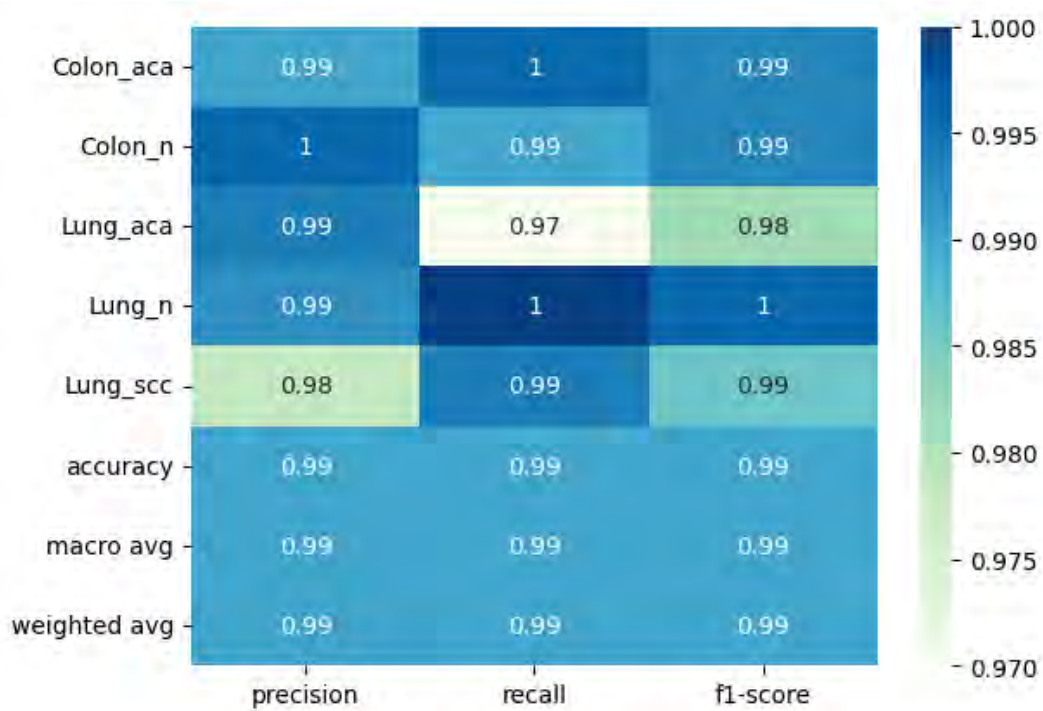


Fig. 4.9: Classification report of DenseNet121

Vision transformer -

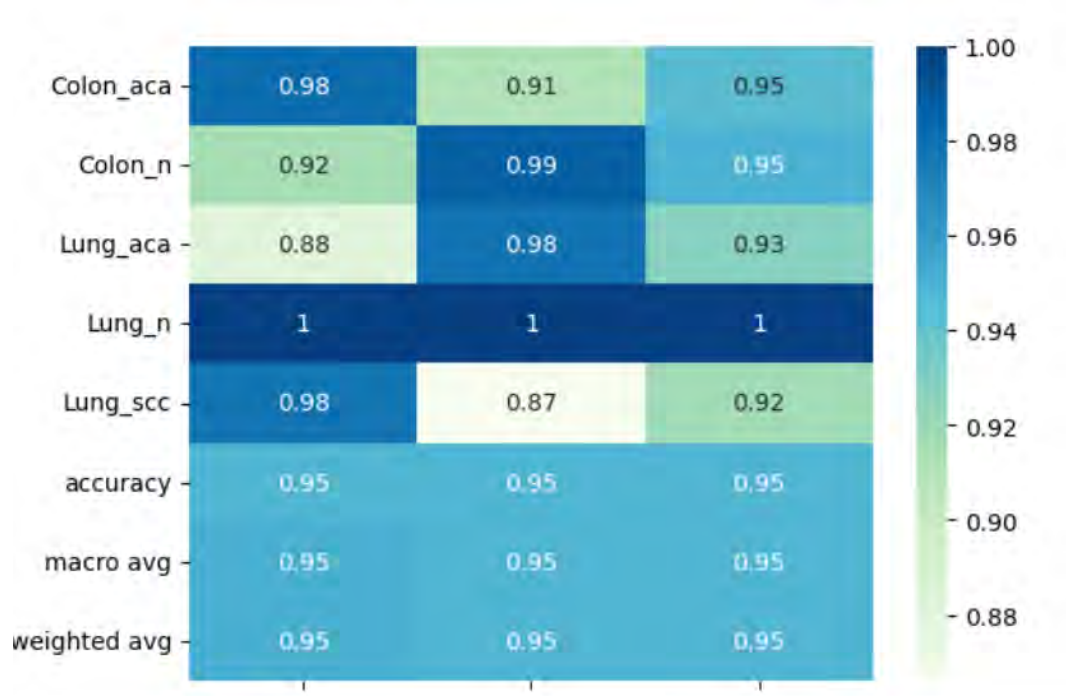


Fig. 4.10: Classification report of Vision transformer

### 4.2.3 Confusion Matrix

VGG16 -

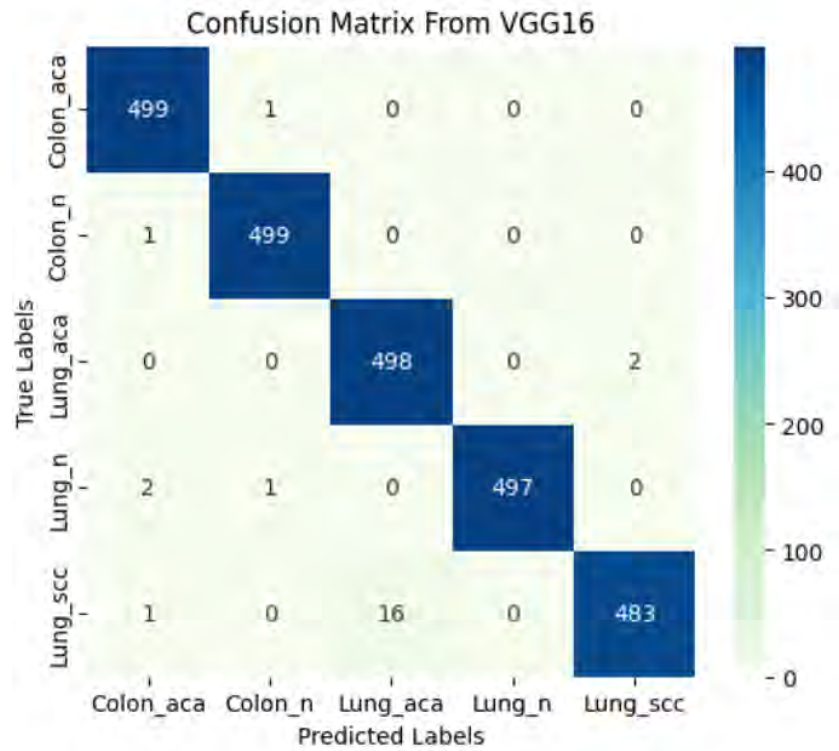


Fig. 4.11: Confusion matrix of VGG16

VGG19 -

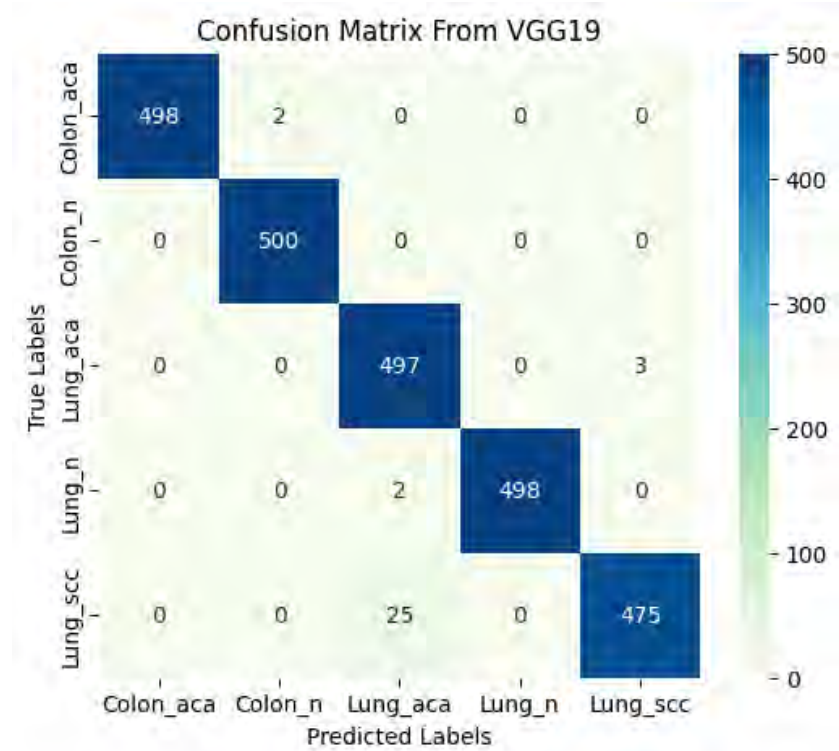


Fig. 4.12: Confusion matrix of VGG19

ResNet50 -

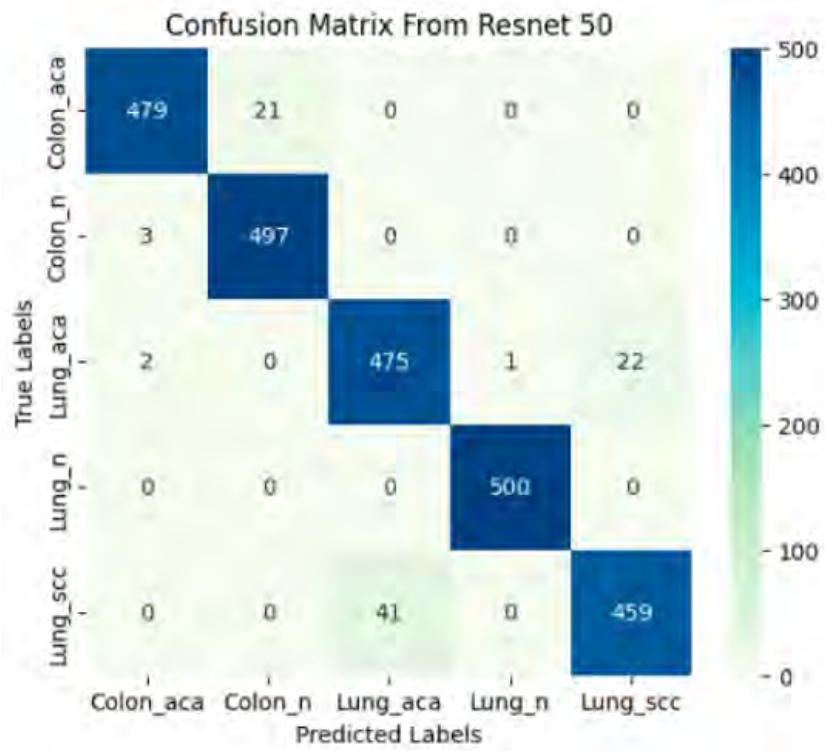


Fig. 4.13: Confusion matrix of ResNet50

DenseNet121 -

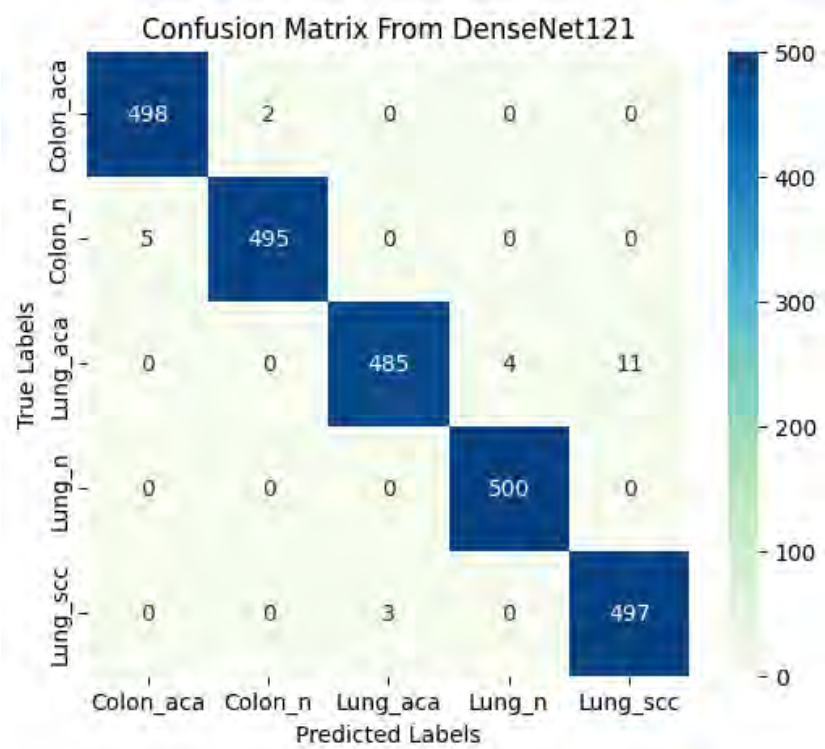


Fig. 4.14: Confusion matrix of DenseNet121

Vision transformer -

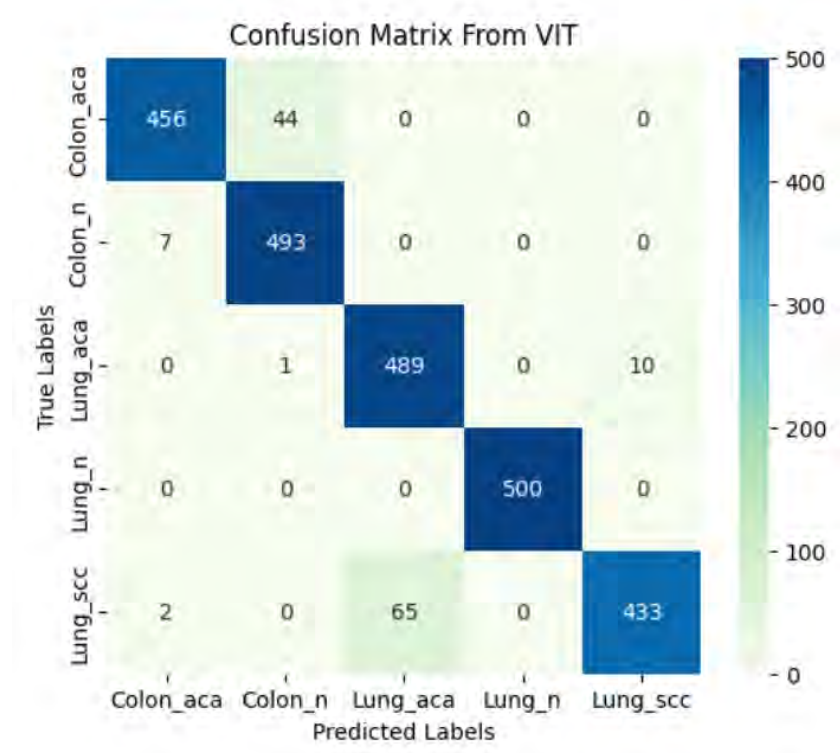


Fig. 4.15: Confusion matrix of Vision transformer



## 4.2.4 Result Analysis & Comparison:

### Result Analysis:

We've employed a range of optimizers including feature tuning techniques for hyperparameter tuning. We experimented with various batch sizes, and among them, 32 batches yielded higher accuracy. We utilized a learning rate of  $1e-5$  and employed the ADAM optimizer in our model training.

Include_Top: False, Weights: None, Pretrained: False, Pretrained_Top: False				
Model Architecture	Batch Size	Learning Rate	Optimizer	Accuracy
VGG-16	32	$1e-5$	ADAM	99.04%
VGG-19	32	$1e-5$	ADAM	98.7%
DenseNet121	32	$1e-5$	ADAM	99%
ResNet50	32	$1e-5$	ADAM	96.4%
Vision Transformer	32	$1e-5$	ADAM	94.8%

### Comparison:

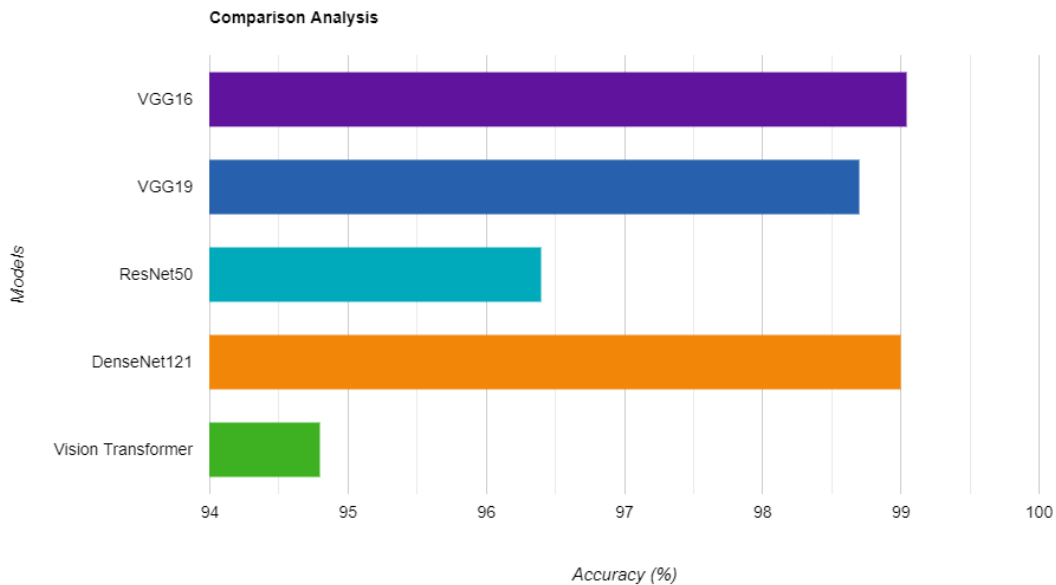


Fig. 4.16: Comparison between model in terms of accuracy

In comparison, while both VGG-16 and DenseNet121 exhibit high accuracy rates, VGG-16 achieved an accuracy of 99.04%, while DenseNet121 achieved the accuracy of 99% for the batch size of 32. Despite delivering the same high accuracy after 50 epochs, our findings show that VGG-16 has been chosen as it seemed the ideal one considering factors such as computational efficiency and sample complexity. The model's superior performance on both the training and validation sets suggests its ability to learn complex patterns in the data while avoiding overfitting. As VGG-16 has given the best performance in model training results comparatively from other models, we have selected this model for next steps.

## 4.2.5 GradCAM Visualization of Individual Model

Grad-CAM images have provided valuable insight into specific regions that the VGG-16 model relies on for classification. These maps effectively highlight key areas on histological slides that significantly affect the predictions of the model. The areas of intensity identified in the heat maps correspond to areas of importance in cellular structure and microphysiology that carry the most weight in the decision-making process of deep tissue. If these features are highlighted, it demonstrates the semantic validity of Grad-CAM in line with expert pathology. Comparison of these highlighted areas with the original slides allows for analytical confirmation, especially when they correspond to established markers and consequently gives confidence in the area of humans the alignment with machine vision is considered reasonable is high. Overall, here, Grad-CAM acts as a bridge, clarifying the rationale behind the model's calculations to localize diagnostic attention. These implicit assumptions contribute to a better understanding of the model's conceptual framework in cancer coding.

Colon\_aca:

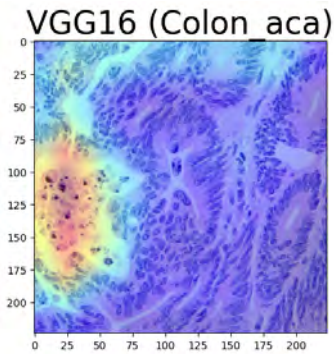


Fig. 4.17: GradCAM Visualization of Colon\_aca

Colon\_n:

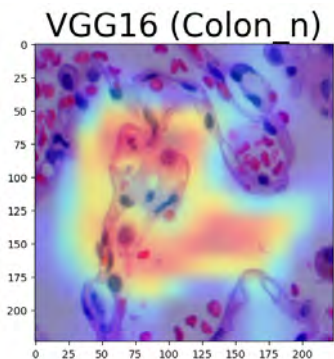


Fig. 4.18: GradCAM Visualization of Colon\_n

Lung\_aca:

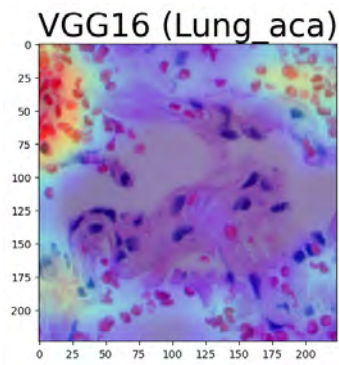


Fig. 4.19: GradCAM Visualization of Lung\_aca

Lung\_n:

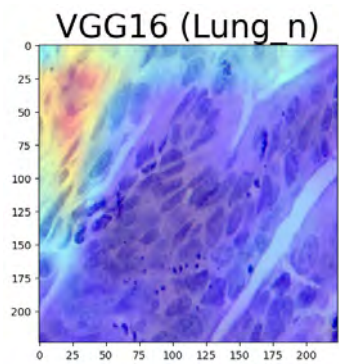


Fig. 4.20: GradCAM Visualization of Lung\_n

Lung\_scc:

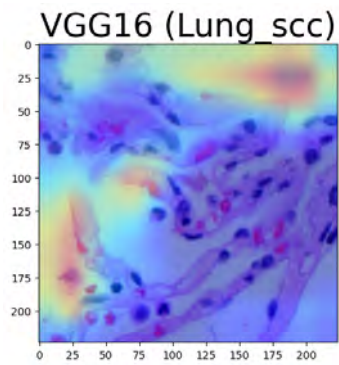


Fig. 4.21: GradCAM Visualization of Lung\_scc

## 4.3 Performance Evaluation of Federated Learning

As we proceed to the federated learning environment, we chose VGG-16 as our base model for this environment. VGG-16 and DenseNet121 gave the best result in comparison to other models we have used for training, evaluating and testing on our overall dataset where we extracted the individual model performances.

### 4.3.1 Result Analysis of Global Model

Model Architecture	Batch Size	Learning Rate	Optimizer	Accuracy
Global Model	32	1e-5	ADAM	89.5%

### 4.3.2 Learning Curves for Global Model

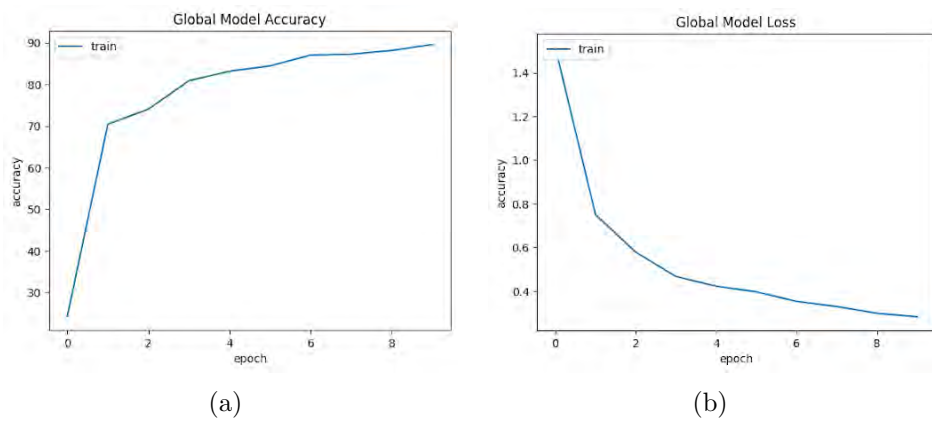


Fig. 4.22: Accuracy and Loss Curves for Global Model

### 4.3.3 Classification Report for Global Model

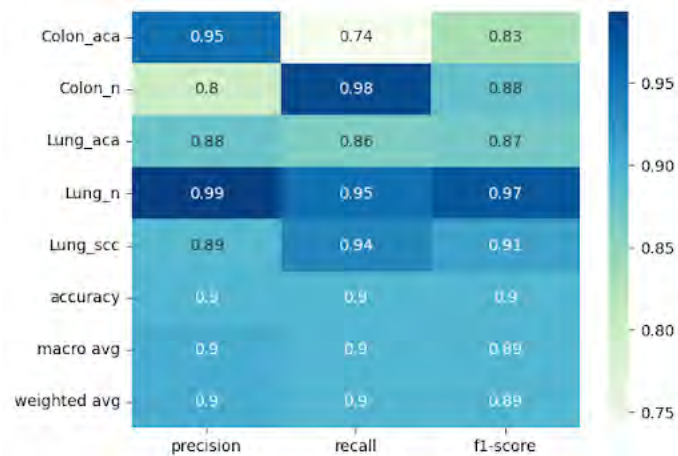


Fig. 4.23: Classification Report for Global Model

### 4.3.4 Confusion Matrix for Global Model

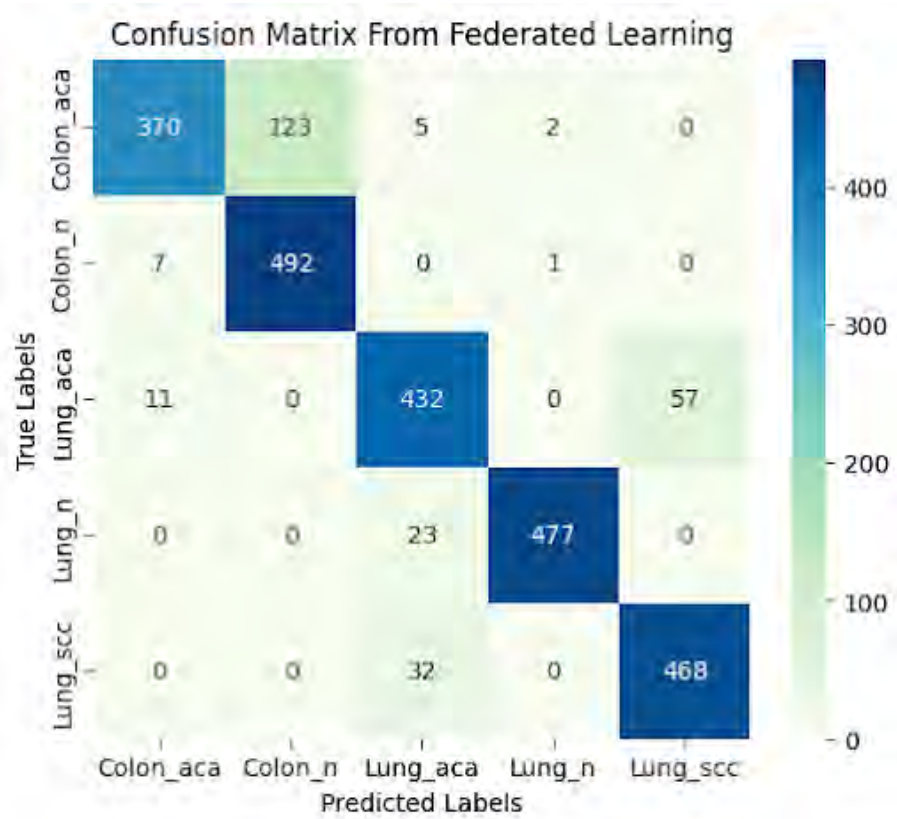


Fig. 4.24: Confusion Matrix for Global Model

### 4.3.5 ROC Curve for Global Model

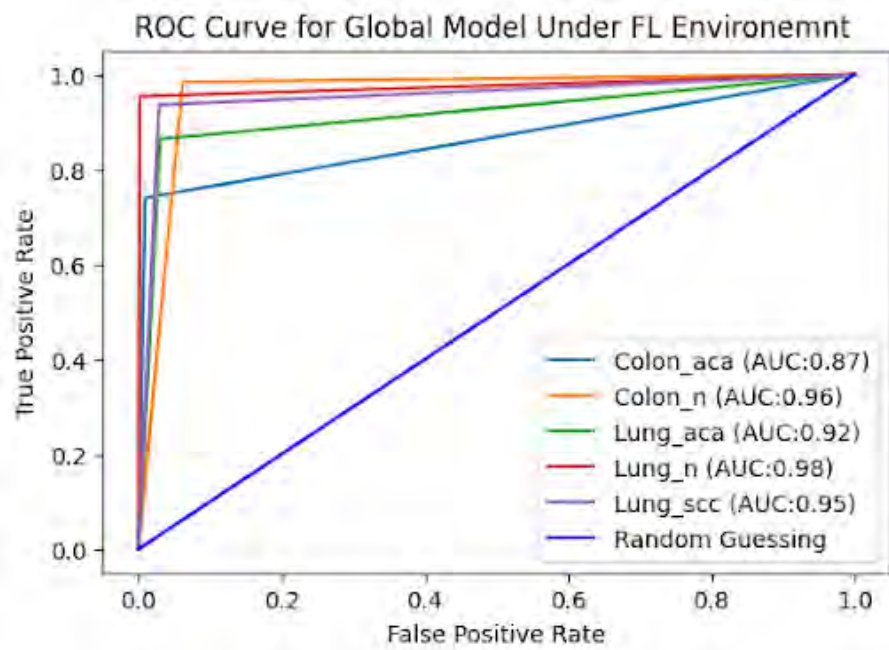


Fig. 4.25: ROC Curve for Global Model

### 4.3.6 GradCAM Visualization of FL Model

Colon\_aca:

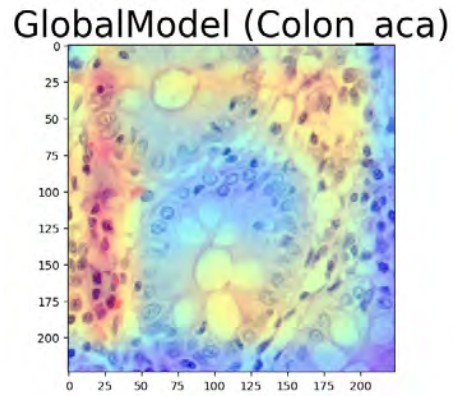


Fig. 4.26: GradCAM Visualization of Colon\_aca

Colon\_n:

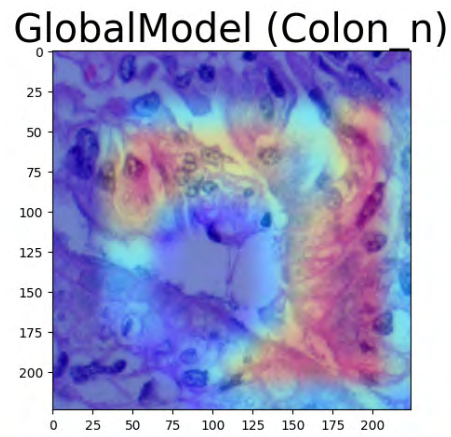


Fig. 4.27: GradCAM Visualization of Colon\_n

Lung\_aca:

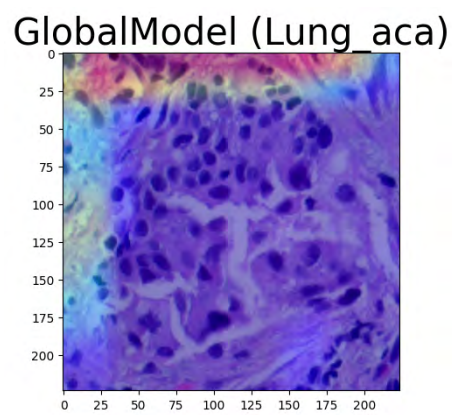


Fig. 4.28: GradCAM Visualization of Lung\_aca

Lung\_n:

GlobalModel (Lung\_n)

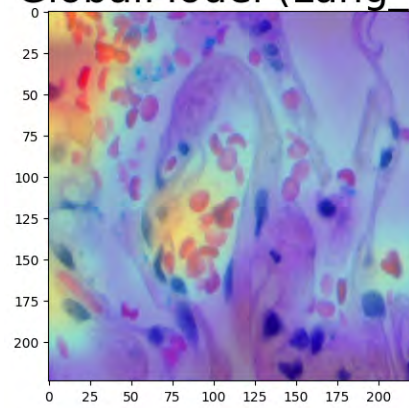


Fig. 4.29: GradCAM Visualization of Lung\_n

Lung\_scc:

GlobalModel (Lung\_scc)

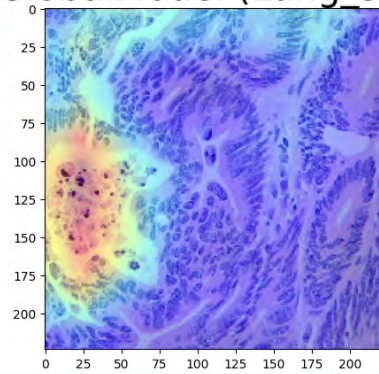
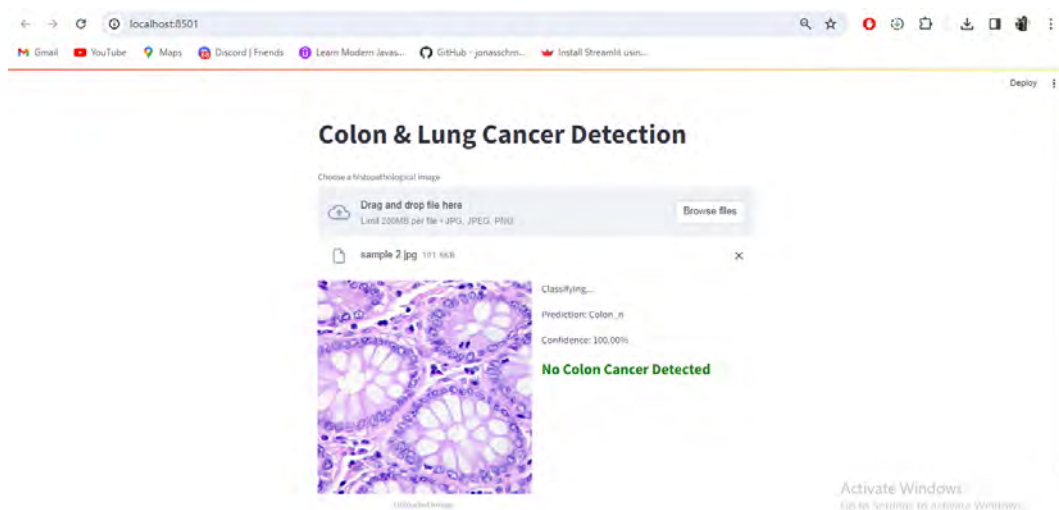
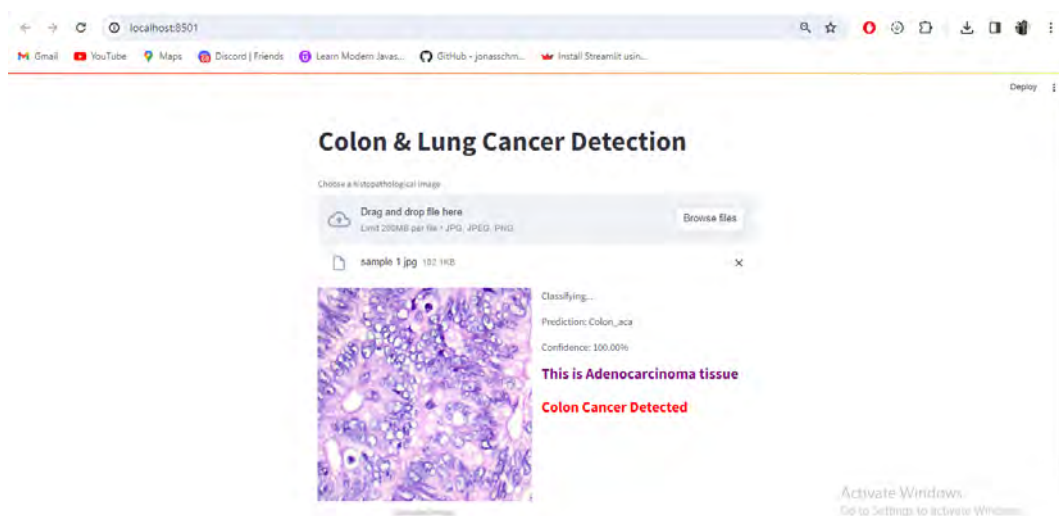


Fig. 4.30: GradCAM Visualization of Lung\_scc

## 4.4 The Web Application “EAI4CC”

The global model has been used to run the web-app system, which was generated by the federated learning environment. The culmination of this process was the development of a functional and effective cancer detection tool. In the course of study, the description of the functionality of the application deals with the use of a method that prompts users to send an image of a suspected infected cell. Using the global model, the application performs detection analysis to determine the true cellular infection. This user-centered approach ensures that research findings are effectively and efficiently integrated into real-world healthcare contexts.

Here are some results from the Web Application -





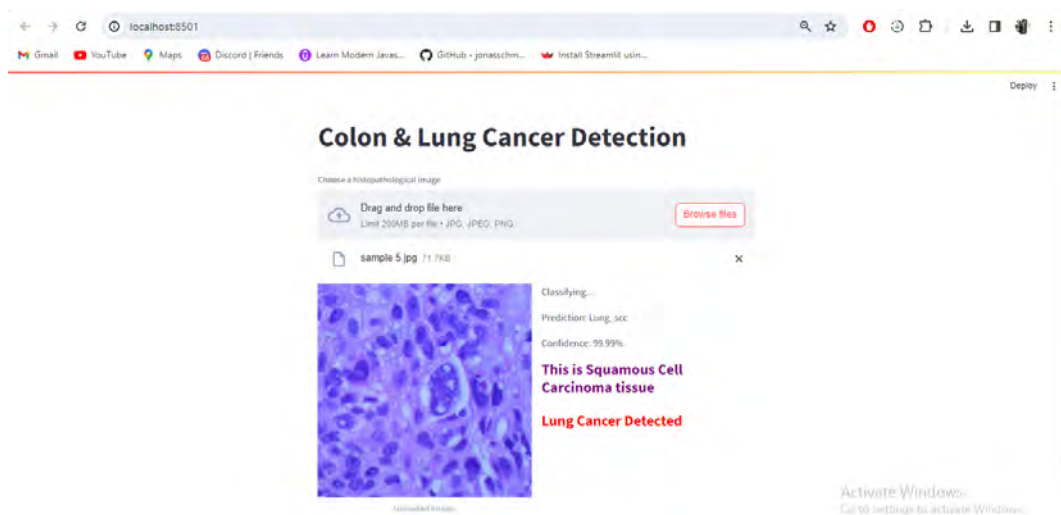
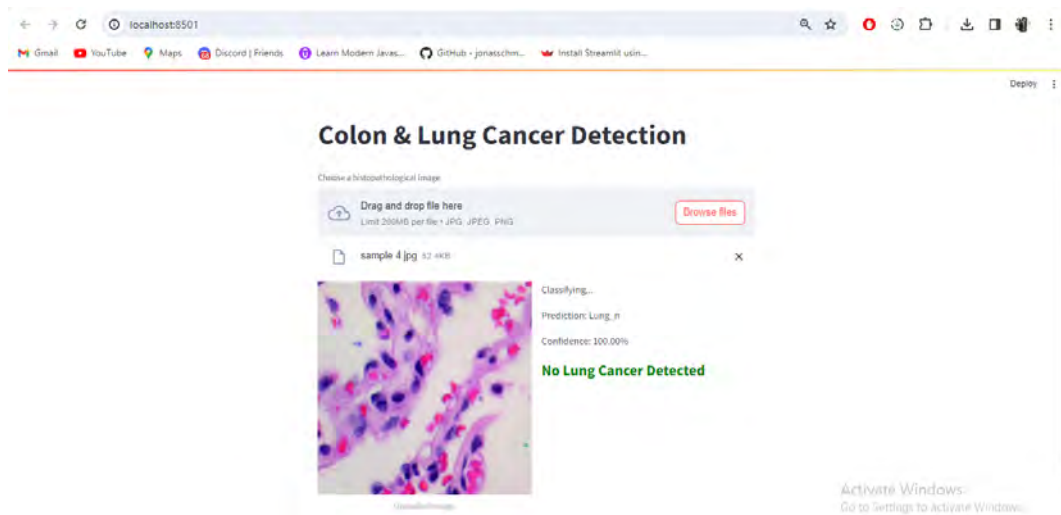
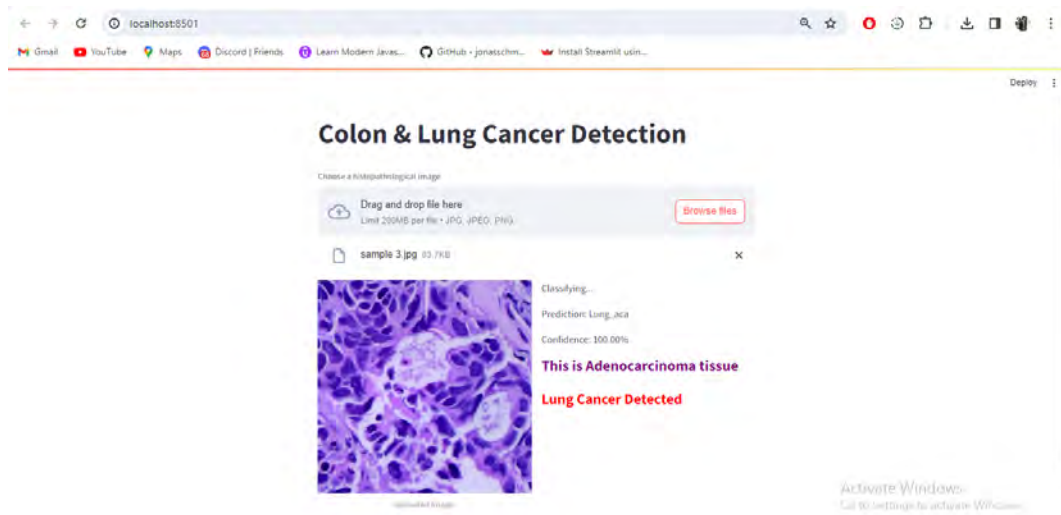


Fig. 4.31: Some test results of Web Application EAI4CC

# Chapter 5

## Conclusion and Future Work

### **Conclusion:**

Colorectal and lung cancer pose a significant global health challenge, with factors such as genetic predisposition, diet, environmental influences, and gastrointestinal inflammation combining to contribute to individual or individual risk factors they have a family history is high Colorectal cancer results from DNA mutations in functional colon cells Acts as a facilitator system for important cellular processes that need to go on. Precise diagnosis include CBC, CMP, etc. Including histopathological examination of tissue from the uterus and lung provide important insights Our research focuses on differentiating between healthy and cancerous tissue. By seamlessly integrating artificial intelligence with deep learning, our system demonstrates improved proficiency in detecting abnormalities in physiological pathology images, producing transformative effects on colorectal and lung cancer diagnosis. Expanding our study to include lung and colorectal cancer highlights their important roles in the broader cancer landscape. Our approach prioritizes genetic traits, environmental factors, and early detection, using state-of-the-art techniques such as Grad-CAM and Transformers. Additionally, the implementation of Federated Learning, designed for security purposes, enhances diagnostic capabilities by predicting patterns and density types in histopathological images, facilitating a nuanced understanding of tissue characteristics. In our pioneering project, we introduced an application that allows users to send images of lung or spleen cells for immediate diagnosis of neurological or cellular pathology. Driven by our strong research efforts, this user-friendly tool is a valuable diagnostic tool for physicians dealing with colorectal and lung cancer capable of assessing tissue status fast and accurately and improves life-saving results.

### **Future work:**

The general direction of our program is to expand the ability to detect cancer through a government program, prioritizing privacy through our emphasis on diversity. Biomarker extraction for staging, global collaboration with healthcare providers, and improved data protection also help improve early detection. In future studies, we plan to evaluate other cancers, which are also histopathologically difficult to evaluate, and pursue staging if data collection progress permits. Our focus extends to developing integrated learning methods, benchmarking aggregation algorithms, and

integrating privacy preservation techniques into our FedHealth platform, aiming to develop standardized protocols designed for collaborative deep learning on medical data. Implementation of image validation for federate learning and also merging more similar kind datasets with the help professionals are also into our plan.

# Bibliography

- [1] Y. Al-Kofahi, W. Lassoued, W. Lee, and B. Roysam, ‘Improved automatic detection and segmentation of cell nuclei in histopathology images,’ *IEEE Transactions on Biomedical Engineering*, vol. 57, no. 4, pp. 841–852, 2009.
- [2] N. Eiamkanitchat, N. Theera-Umpon, and S. Auephanwiriyakul, ‘Colon tumor microarray classification using neural network with feature selection and rule-based classification,’ in *Advances in Neural Network Research and Applications*, Springer, 2010, pp. 363–372.
- [3] A. Chaddad, C. Tanougast, A. Dandache, A. Al Houseini, and A. Bouridane, ‘Improving of colon cancer cells detection based on haralick’s features on segmented histopathological images,’ in *2011 IEEE international conference on computer applications and industrial electronics (ICCAIE)*, IEEE, 2011, pp. 87–90.
- [4] K. Nguyen, A. K. Jain, and B. Sabata, ‘Prostate cancer detection: Fusion of cytological and textural features,’ *Journal of pathology informatics*, vol. 2, no. 2, p. 3, 2011.
- [5] Y. Xu, L. Jiao, S. Wang, *et al.*, ‘Multi-label classification for colon cancer using histopathological images,’ *Microscopy Research and Technique*, vol. 76, no. 12, pp. 1266–1277, 2013.
- [6] F. Iandola, M. Moskewicz, S. Karayev, R. Girshick, T. Darrell, and K. Keutzer, *Densenet: Implementing efficient convnet descriptor pyramids*, 2014. arXiv: 1404.1869 [cs.CV].
- [7] K. He, X. Zhang, S. Ren, and J. Sun, *Deep residual learning for image recognition*, 2015. arXiv: 1512.03385 [cs.CV].
- [8] J. Konečný, H. B. McMahan, F. X. Yu, P. Richtárik, A. T. Suresh, and D. Bacon, *Federated learning: Strategies for improving communication efficiency*, 2017. arXiv: 1610.05492 [cs.LG].
- [9] F. Ponzio, E. Macii, E. Ficarra, and S. Di Cataldo, ‘Colorectal cancer classification using deep convolutional networks,’ in *Proceedings of the 11th international joint conference on biomedical engineering systems and technologies*, vol. 2, 2018, pp. 58–66.
- [10] M. A. Rahman and R. C. Muniyandi, ‘Feature selection from colon cancer dataset for cancer classification using artificial neural network,’ *International Journal on Advanced Science, Engineering and Information Technology*, vol. 8, no. 4-2, pp. 1387–1393, 2018.

- [11] A. A. Borkowski, M. M. Bui, L. B. Thomas, C. P. Wilson, L. A. DeLand, and S. M. Mastorides, *Lung and colon cancer histopathological image dataset (lc25000)*, 2019. arXiv: 1912.12142 [eess.IV].
- [12] R. R. Selvaraju, M. Cogswell, A. Das, R. Vedantam, D. Parikh, and D. Batra, ‘Grad-cam: Visual explanations from deep networks via gradient-based localization,’ *International Journal of Computer Vision*, vol. 128, no. 2, pp. 336–359, Oct. 2019, ISSN: 1573-1405. DOI: 10.1007/s11263-019-01228-7. [Online]. Available: <http://dx.doi.org/10.1007/s11263-019-01228-7>.
- [13] S. Tammina, ‘Transfer learning using vgg-16 with deep convolutional neural network for classifying images,’ *International Journal of Scientific and Research Publications (IJSRP)*, vol. 9, no. 10, 2019. DOI: 10.29322/ijsrp.9.10.2019.p9420.
- [14] S. Garg and S. Garg, ‘Prediction of lung and colon cancer through analysis of histopathological images by utilizing pre-trained cnn models with visualization of class activation and saliency maps,’ in *2020 3rd Artificial Intelligence and Cloud Computing Conference*, 2020, pp. 38–45.
- [15] P. Sabol, P. Sinčák, P. Hartono, *et al.*, ‘Explainable classifier for improving the accountability in decision-making for colorectal cancer diagnosis from histopathological images,’ *Journal of biomedical informatics*, vol. 109, p. 103 523, 2020.
- [16] D. Wang, J. Xu, Z. Zhang, *et al.*, ‘Evaluation of rectal cancer circumferential resection margin using faster region-based convolutional neural network in high-resolution magnetic resonance images,’ *Diseases of the Colon & Rectum*, vol. 63, no. 2, pp. 143–151, 2020.
- [17] J. Xiao, J. Wang, S. Cao, and B. Li, ‘Application of a novel and improved vgg-19 network in the detection of workers wearing masks,’ *Journal of Physics: Conference Series*, vol. 1518, no. 1, p. 012 041, Apr. 2020. DOI: 10.1088/1742-6596/1518/1/012041. [Online]. Available: <https://dx.doi.org/10.1088/1742-6596/1518/1/012041>.
- [18] M. Adnan, S. Kalra, J. C. Cresswell, G. W. Taylor, and H. Tizhoosh, *Federated learning and differential privacy for medical image analysis*, 2021. DOI: 10.21203/rs.3.rs-1005694/v1. [Online]. Available: <https://www.nature.com/articles/s41598-022-05539-7.pdf>.
- [19] A. Ali and C. Britto, ‘Performance analysis of colon cancer using neural networks,’ Sep. 2021.
- [20] K. Wu, H. Peng, M. Chen, J. Fu, and H. Chao, ‘Rethinking and improving relative position encoding for vision transformer,’ in *Proceedings of the IEEE/CVF International Conference on Computer Vision (ICCV)*, Oct. 2021, pp. 10 033–10 041.
- [21] Apr. 2022. [Online]. Available: <https://www.wcrf.org/cancer-trends/worldwide-cancer-data/>.
- [22] B. L. Y. Agbley, J. Li, A. U. Haq, *et al.*, ‘Federated approach for lung and colon cancer classification,’ in *2022 19th International Computer Conference on Wavelet Active Media Technology and Information Processing (ICCWAMTIP)*, 2022, pp. 1–8. DOI: 10.1109/ICCWAMTIP56608.2022.10016590.

- [23] S. Bharati, M. R. Mondal, P. Podder, and S. Prasath, ‘Federated learning: Applications, challenges and future directions,’ *International Journal of Hybrid Intelligent Systems*, vol. 18, pp. 19–35, Apr. 2022. DOI: 10.3233/HIS-220006.
- [24] *Ca: A cancer journal for clinicians*, <https://acsjournals.onlinelibrary.wiley.com/doi/10.3322/caac.21708>, Jan. 2022.
- [25] A. H. Chehade, N. Abdallah, J.-M. Marion, M. Oueidat, and P. Chauvet, ‘Lung and colon cancer classification using medical imaging: A feature engineering approach,’ 2022.
- [26] A. Chowdhury, H. Kassem, N. Padoy, R. Umeton, and A. Karargyris, ‘A review of medical federated learning: Applications in oncology and cancer research,’ in *Brainlesion: Glioma, Multiple Sclerosis, Stroke and Traumatic Brain Injuries*, A. Crimi and S. Bakas, Eds., Cham: Springer International Publishing, 2022, pp. 3–24, ISBN: 978-3-031-08999-2.
- [27] S. d. Cruz, A. K. Ribeiro, M. d. Pinheiro, V. C. Carneiro, L. M. Neves, and S. R. Carneiro, ‘Five-year survival rate and prognostic factors in women with breast cancer treated at a reference hospital in the brazilian amazon,’ *PLOS ONE*, vol. 17, no. 11, 2022. DOI: 10.1371/journal.pone.0277194.
- [28] I. Hasan, S. Ali, H. Rahman, and K. Islam, ‘Automated detection and characterization of colon cancer with deep convolutional neural networks,’ *Journal of Healthcare Engineering*, vol. 2022, 2022.
- [29] I. D. Irawati, I. A. Larasaty, and S. Hadiyoso, ‘Comparison of convolution neural network architecture for colon cancer classification.,’ *International Journal of Online & Biomedical Engineering*, vol. 18, no. 3, 2022.
- [30] L. Li, N. Xie, and S. Yuan, ‘A federated learning framework for breast cancer histopathological image classification,’ *Electronics*, vol. 11, no. 22, 2022, ISSN: 2079-9292. DOI: 10.3390/electronics11223767. [Online]. Available: <https://www.mdpi.com/2079-9292/11/22/3767>.
- [31] A. Zafar and M. Nadeem, ‘Performance evaluation of 2d cnn optimizers for lung and colon cancer image classification,’ in *Proceedings of International Conference on Communication and Artificial Intelligence*, Springer, 2022, pp. 515–525.
- [32] M. Moshawrab, M. Adda, A. Bouzouane, H. Ibrahim, and A. Raad, ‘Reviewing federated machine learning and its use in diseases prediction,’ *Sensors (Basel, Switzerland)*, vol. 23, Feb. 2023. DOI: 10.3390/s23042112.
- [33] S. Nazir and M. Kaleem, ‘Federated learning for medical image analysis with deep neural networks,’ *Diagnostics*, vol. 13, no. 9, p. 1532, 2023. DOI: 10.3390/diagnostics13091532.
- [34] I. American Cancer Society, *Key statistics for colorectal cancer*, 2024. [Online]. Available: <https://www.cancer.org/cancer/types/colon-rectal-cancer/about/key-statistics.html#:~:text=In%20the%20United%20States%2C%20colorectal,about%2052%2C550%20deaths%20during%202023>.
- [35] *Colorectal cancer: Colorectal cancer epidemiology: Incidence, mortality, survival, and risk factors - pmc*, <https://ncbi.nlm.nih.gov/pmc/articles/PMC2796096/>, Sep. 2024.

- [36] *Transformation from non-small-cell lung cancer to small-cell lung cancer: Molecular drivers and cells of origin - pmc*, Sep. 2024. [Online]. Available: <https://www.ncbi.nlm.nih.gov/pmc/articles/PMC4470698/#:~:text=WHO%20classifies%20lung%20cancer%20into,%2C%20and%20large%2Dcell%20carcinoma.>
- [37] G. Boesch, *Deep residual networks (resnet, resnet50) – 2023 guide*, <https://viso.ai/deep-learning/resnet-residual-neural-network/>, Accessed: 2023.

# Appendix

Paper Title	Models Used	Performance
Early Stage Detection and Classification of Colon Cancer using Deep Learning and Explainable AI on Histopathological Images	<ul style="list-style-type: none"> <li>• ResNet50</li> <li>• VGG-16</li> <li>• Base Model (custom/unspecified model)</li> </ul>	<p><b>ResNet50 Results:</b>            Batch Size: 64            Learning Rate: 0.01            Accuracy: 92.1%</p> <p>Batch Size: 64            Learning Rate: 0.001            Accuracy: 96.7%</p> <p><b>VGG-16 Results:</b>            Batch Size: 64            Learning Rate: 0.01            Accuracy: 95.4%</p> <p>Batch Size: 64            Learning Rate: 0.001            Accuracy: 96.7%</p> <p><b>Base Model Results:</b>            Batch Size: 64            Learning Rate: 0.01            Accuracy: 94.5%</p> <p>Batch Size: 64            Learning Rate: 0.001            Accuracy: 96.2%</p>



<p>Automated Detection and Characterization of Colon Cancer with Deep Convolutional Neural Networks</p>	<ul style="list-style-type: none"> <li>• VGG-16</li> <li>• ResNet101V2</li> <li>• EfficientNetB0</li> <li>• DenseNet121</li> <li>• MobileNetV2</li> <li>• ResNet50</li> <li>• Proposed DCNN (Deep Convolutional Neural Network)</li> </ul>	<p><b>The model proposed DCNN achieved the best performance with:</b>  Precision: 100%  Recall: 99.59%  F1-score: 99.80%  Training Accuracy:99.87%  Testing Accuracy: Not reported</p> <p><b>VGG-16 Results:</b>  Testing Accuracy: 92.90%</p> <p><b>ResNet101V2 Results:</b>  Testing Accuracy: 90.45%</p> <p><b>EfficientNetB0 Results:</b>  Testing Accuracy: 91.80%</p> <p><b>DenseNet121 Results:</b>  Testing Accuracy: 91.10%</p> <p><b>MobileNetV2 Results:</b>  Testing Accuracy: 81.26%</p> <p><b>ResNet50 Results:</b>  Testing Accuracy: 89.80%</p>
---	--	---

Lung and colon cancer classification using medical imaging: a feature engineering approach LC25000 dataset	<ul style="list-style-type: none"> <li>• XGBoost</li> <li>• SVM (Support Vector Machine)</li> <li>• RF (Random Forest)</li> <li>• LDA (Linear Discriminant Analysis)</li> <li>• MLP (Multilayer Perceptron)</li> <li>• LightGBM</li> </ul>	<p><b>The XGBoost model achieved the best performance with:</b></p> <p>Accuracy: 99%</p> <p>F1-score: 98.8%</p>
Prostate cancer detection: Fusion of cytological and textural features	Does not mention any specific machine learning or deep learning models used for classifying or detecting prostate cancer.	there is no information provided about which machine/deep learning models were used in those past studies, or a comparison of results between models.
Explainable classifier for improving the accountability in decision-making for colorectal cancer diagnosis from histopathological images	<ul style="list-style-type: none"> <li>• Explainable classifier</li> <li>• Cumulative Fuzzy Class Membership Criterion (CFCMC)</li> </ul>	
Feature Selection from Colon Cancer Dataset for Cancer Classification using Artificial Neural Network	<ul style="list-style-type: none"> <li>• Artificial Neural Networks (ANNs)</li> </ul> <p>[No other machine learning models were used]</p>	<p><b>Cross-Entropy:</b> 3.2004</p> <p><b>Percent of Error:</b> 1.6129%</p> <p><b>Classification Accuracy:</b> 98.4%</p>

<p>Multi-label classification for colon cancer using histopathological images</p>	<ul style="list-style-type: none"> <li>• One-Against-All SVM (OAA SVM)</li> <li>• One-Against-One SVM (OAO SVM)</li> <li>• Multi-Structure SVM</li> <li>• Multi-Label Model (proposed method)</li> </ul>	<p><b>The proposed multi-label model achieved the best performance with:</b></p> <p><b>Precision:</b> 73.7%  <b>Recall:</b> 68.2%  <b>F-measure:</b> 70.8%</p> <p>[The multi-label model outperformed the other SVM models based on precision, recall and F-measure.]</p>
<p>A Federated Learning Framework for Breast Cancer Histopathological Image Classification</p>	<ul style="list-style-type: none"> <li>• ResNet-152</li> <li>• DenseNet-201</li> <li>• MobileNet-v2-100</li> <li>• EfficientNet-b7</li> </ul>	<p><b>ResNet-152 achieved the best</b>  ACC_IL of 84.39%  ACC_PL of 86.01% and  F1 score of 67.45% using federated learning.</p> <p><b>DenseNet-201 achieved the second best with</b>  ACC_IL of 91.06%  ACC_PL of 91.87% and  F1 score of 84.97%</p> <p><b>MobileNet-v2-100 was third best with</b>  ACC_IL 87.38%  ACC_PL 86.17% and  F1 77.38%.</p> <p><b>EfficientNet-b7 performed least well likely because of fewer training rounds, achieving</b>  ACC_IL 84.02% ACC_PL 84.09% and F1 72.78%.</p>

<p>Federated learning and differential privacy for medical image analysis</p>	<ul style="list-style-type: none"> <li>• MEM (Memory Enhanced MIL)</li> <li>• Dense Net model</li> </ul>	<p><b>federated learning method</b> achieves privacy budget <math>\epsilon = 2.9</math> with <math>\delta = 0.0001</math> based on the differential privacy accountant.</p>
<p>Federated Learning for Medical Image Analysis with Deep Neural Networks</p>	<ul style="list-style-type: none"> <li>• <b>COVID-19 detection:</b> ResNet18, ResNet50, VGG16, DenseNet121, InceptionV3, Xception, Capsule Networks, Transformer models</li> <li>• <b>Pneumonia classification:</b> Custom CNN models</li> <li>• <b>Breast cancer:</b> DenseNet-121 for density classification, Res Net for histopathology image analysis</li> <li>• <b>Brain tumor analysis:</b> U-Net, DenseNet121, VGG19, Inception V3</li> <li>• <b>Colorectal cancer:</b> GAN models</li> <li>• <b>Prostate and lung cancer:</b> CNN models, EfficientNetB7, Hypernetworks</li> <li>• <b>Key CNN architectures used:</b> Res Net, Dense Net, Inception, VGG, Capsule Networks</li> </ul>	<ul style="list-style-type: none"> <li>• <b>ResNet18 model with Distance-based Outlier Suppression (DOS)</b> provided protection against poisoning attacks on federated learning.</li> <li>• <b>Randomization mechanism with Gaussian/Laplace noise</b> added to model weights protected against gradient inversion attacks but reduced model accuracy.</li> <li>• <b>Homomorphic encryption with masks</b> provided local model privacy but had computational overhead.</li> <li>• <b>Differential privacy techniques on Attention based MIL,</b> custom COVID-19 model, and histopathology images provided data privacy guarantees.</li> </ul>

		<ul style="list-style-type: none"> <li>• <b>Augmented Multi-Party Computation (AMPC) with encryption</b> protected against model leakages.</li> <li>• <b>Custom CNN model</b> handled intermittent clients and reduced computing time over centralized learning.</li> <li>• <b>Contrastive learning frameworks</b> like MOON and FMTLJD improved model training with unlabeled data.</li> <li>• <b>Incremental learning with exemplars</b> reduced time and space complexity for continuous medical data streams.</li> </ul>
<p>A Review of Medical Federated Learning: Applications in Oncology and Cancer Research</p>	<ul style="list-style-type: none"> <li>• U-Net, DenseNet121, VGG19, Inception V3</li> <li>• ResNet</li> <li>• DenseNet-121</li> <li>• Capsule Networks</li> <li>• Transformer models</li> <li>• GAN models</li> </ul>	<p><b>Federated deep learning</b> has shown promise for collaborative training on decentralized medical data, while addressing data privacy, distributional skew, and confidentiality issues. Careful model design and encryption techniques allow achieving performance close to centralized training.</p>

	<ul style="list-style-type: none"> <li>• CNN models like CusFL</li> <li>• Hypernetworks</li> <li>• Homomorphic encryption</li> <li>• Differential privacy techniques</li> </ul>	
<p>Federated learning: Applications, challenges and future directions</p>	<ul style="list-style-type: none"> <li>• Convolutional neural networks (CNNs)</li> <li>• Recurrent neural networks (RNNs)</li> <li>• Multilayer perceptrons (MLPs)</li> <li>• Logistic regression (LR)</li> <li>• Neural networks (NNs)</li> <li>• LASSO, linear regression with regularization (LRR) -</li> <li>• Autoencoders</li> <li>• Natural language processing (NLP)</li> <li>• Tensor factorization (TF)</li> </ul>	<ul style="list-style-type: none"> <li>• <b>Convolutional neural networks (CNNs):</b> Used for COVID-19 detection from CT images, cancer diagnosis from medical images, activity recognition. Provide high accuracy for image classification tasks.</li> <li>• <b>Recurrent neural networks (RNNs):</b> Used for predicting preterm birth risk from time-series data. Capture temporal dependencies well.</li> <li>• <b>Multilayer perceptrons (MLPs):</b> Used for mortality prediction in ICU patients. Simple feedforward networks that can model complex functions.</li> </ul>

		<ul style="list-style-type: none"> <li>• <b>Logistic regression (LR):</b> Used for hospitalization prediction, mortality prediction. Linear model well-suited for binary classification problems.</li> <li>• <b>Neural networks (NNs) in general:</b> Used for arrhythmia detection, mortality prediction. Non-linear models that can approximate complex functions.</li> <li>• <b>LASSO, linear regression with regularization (LRR):</b> Used for mortality prediction in COVID-19. Regularized linear models good for feature selection.</li> <li>• <b>Autoencoders:</b> Used for patient representation learning from EHR data. Unsupervised approach to learn compressed representations.</li> <li>• <b>Natural language processing (NLP) models:</b> Used for phenotyping tasks from clinical text. Learn from unstructured notes and reports.</li> </ul>
--	--	---

		<ul style="list-style-type: none"> <li>• <b>Tensor factorization (TF):</b> Used for computational phenotyping from EHR data. Capture multi-way interactions in tensor data</li> </ul>
Colorectal Cancer Classification using Deep Convolutional Networks - An Experimental Study	<ul style="list-style-type: none"> <li>• VGG16</li> <li>• Pre-trained CNN</li> <li>• SVM classifier</li> </ul>	<ul style="list-style-type: none"> <li>• <b>VGG16 architecture achieved</b> around 90% accuracy.</li> <li>• <b>An SVM classifier achieved</b> 96.5% accuracy.</li> <li>• <b>Pre-trained CNN on the colorectal images further improved</b> accuracy to 96.8%.</li> </ul>
Prediction of lung and colon cancer through analysis of histopathological images by utilizing pre-trained CNN models with visualization of class activation and saliency maps	<ul style="list-style-type: none"> <li>• VGG16</li> <li>• NASNetMobile</li> <li>• InceptionV3</li> <li>• InceptionResNetV2</li> <li>• ResNet50</li> <li>• Xception</li> <li>• MobileNet</li> <li>• DenseNet169</li> </ul>	<ul style="list-style-type: none"> <li>• All eight models achieved noteworthy results.</li> <li>• <b>Accuracy ranged from 96% to 100%.</b></li> </ul>



<p>Comparison of convolution neural network architecture for colon cancer classification</p>	<ul style="list-style-type: none"> <li>• VGG16</li> <li>• VGG19</li> <li>• ResNet101</li> <li>• ResNet152</li> <li>• MobileNetV2</li> <li>• DenseNet201</li> <li>• InceptionV3</li> </ul>	<ul style="list-style-type: none"> <li>• <b>VGG16:</b> Precision - 99% Recall - 99% F1-score - 99% Accuracy - 99%</li> <li>• <b>VGG19:</b> Precision - 100% Recall - 100% F1-score - 100% Accuracy - 100%</li> <li>• <b>ResNet101:</b> Precision - 100% Recall - 100% F1-score - 100% Accuracy - 100%</li> <li>• <b>ResNet152:</b> Precision - 100% Recall - 100% F1-score - 100% Accuracy - 100%</li> <li>• <b>MobileNetV2:</b> Precision - 96% Recall - 96% F1-score - 96% Accuracy - 96%</li> <li>• <b>DenseNet201:</b> Precision - 93% Recall - 93% F1-score - 93% Accuracy - 93%</li> <li>• <b>InceptionV3:</b> Precision - 89% Recall - 89% F1-score - 89% Accuracy - 89%</li> </ul>
--	---	--